

RANDOM CONNECTION HYPERGRAPHS

MORTEN BRUN, CHRISTIAN HIRSCH, PETER JUHASZ, AND MORITZ OTTO

ABSTRACT. In this paper, we introduce a novel model for random hypergraphs based on weighted random connection models. In accordance with the standard theory for hypergraphs, this model is constructed from a bipartite graph. In our stochastic model, both vertex sets of this bipartite graph form marked Poisson point processes and the connection radius is inversely proportional to a product of suitable powers of the marks. Hence, our model is a common generalization of weighted random connection models and AB random geometric graphs. For this hypergraph model, we investigate the limit theory of a variety of graph-theoretic and topological characteristics such as higher-order degree distribution, Betti numbers of the associated Dowker complex as well as simplex counts. In particular, for the latter quantity we identify regimes of convergence to normal and to stable distribution depending on the heavy-tailedness of the weight distribution. We conclude our investigation by a simulation study and an application to the collaboration network extracted from the arXiv dataset.

1. INTRODUCTION

Since the seminal work of Barabási and Albert [1], the study of complex networks has become a very active field of research. The main reason for this is that many real-world systems can be represented as networks, where the nodes represent the elements of the system and the links represent the interactions between them. Examples of such systems include the Internet, social networks, and biological networks, among others. The study of complex networks has led to the development of new tools and methods to analyze and model the structure and dynamics of these systems.

The popularity of the complex network models can be explained by their ability to capture the main features of real-world networks such as the presence of a scale-free degree distribution, and the small-world property, which means that the average distance between any two nodes in the network is small. Despite these promising results, the most basic complex network models have difficulties in capturing clustering structures that are essential in a variety of application domains. An elegant approach for implementing these clustering effects works by embedding the network nodes in a suitable ambient space so that nearby nodes have a greater tendency to be connected. This geometric embedding therefore encourages the formation of clusters of nodes in a spatial vicinity. While there are a variety of different ways to endow complex networks with a spatial structure, one of the most elegant and mathematically tractable approaches are the age-dependent random connection models (ADRCM) in [10, 12]. These models make it possible to combine a geometric embedding with possibly heavy-tailed vertex weights that can create a hierarchy of hubs that is often observed in real data. This idea also lies at the core of kernel-based networks as considered in [11, 16].

Besides the spatial structure, another important advantage of the ADRCM is that it can be used to model higher-order interactions in complex networks. For instance, in the context of collaboration networks, scientific papers often involve more than one or two authors, thereby illustrating the need to go beyond binary networks. One of the challenges when investigating higher-order networks is that their topology can become highly complicated, which is why tools from the field of algebraic topology are now being used in the context of network analysis. For instance, [23] considered a higher-order model for preferential attachment and could compute the asymptotic growth rate of expected Betti numbers. Moreover, in an earlier work, we studied the potential of the ADRCM as a model for arXiv collaboration data from different fields [14].

While the ADRCM is an exciting model for scale-free networks with a spatial structure, it is too coarse to capture some key features in collaboration networks. Indeed, from the ADRCM, we can tell whether two scientists have collaborated, but there is no way to decide on how many papers they have written together. To deal with this shortcoming, we now propose a spatial hypergraph structure that we call *random connection hypergraph model (RCHM)*. This hypergraph, which we think of a collection of subsets of vertices, will be defined through its incidence graph, i.e., the bipartite graph whose two vertex sets are given by the set of

hypergraph vertices and relations, respectively [3]. In our setting, this bipartite graph has vertex sets given by the authors and documents, respectively with an edge in the bipartite graph indicating that an author has collaborated in a document.

On the model side, the RCHM removes one of the key drawbacks from the ADRCM, namely that the latter does not allow to capture the number of documents that a collection of authors have collaborated on. Despite this improvement, we show that the RCHM remains mathematically tractable. Indeed, we can recover many of the central higher-order characteristics considered in [14] such as higher-order degree distributions, simplex counts and Betti numbers. However, often the bipartite structure induces additional complexities which often requires substantially more involved mathematical machinery compared to the ADRCM. Surprisingly, in the case of simplex counts, the bipartite structure allows us to go further than the ADRCM.

Hence, the main contributions of this manuscript are the following:

- We introduce the RCHM, a higher-order model for bipartite networks. Note that in the setting of traditional spatial networks, the *AB random geometric graphs* are an intensively studied model [7, 15, 19, 24]. However, while previously the bipartite AB random geometric bipartite graphs have received substantial attention in telecommunication networks, they are not suited for collaboration networks as it is not scale free. To the best of our knowledge, the RCHM is the first spatial model applicable to scale free bipartite networks.
- While the bipartite structure of the RCHM induces additional complexities, we show that the RCHM is mathematically tractable. In fact, surprisingly, in the case of simplex counts, the bipartite structure allows us to go further than the ADRCM. We note that the triangle count is of high interest in the context of complex networks since it is intimately related to the clustering coefficients. Both for geometric and combinatorial network models, the clustering coefficient has recently been the topic of intense research [25, 26].
- We illustrate the usefulness of our asymptotic results in finite sample sizes through an extensive simulation study. Finally, we also compare the model to real-world data from the arXiv network.

The rest of the manuscript is organized as follows. In Section 2, we introduce the RCHM and discuss its main properties. We also present the main results of the manuscript. Sections 3 – 8 are devoted to the proofs of the main results. Next, in Section 8 we illustrate the applicability of our asymptotic results in finite sample sizes through an extensive simulation study. Finally, in Section 9, we compare the model to real-world data from the arXiv network.

2. MODEL AND MAIN RESULTS

We work on the space $\mathbb{S} := \mathbb{R} \times [0, 1]$ and interpret \mathbb{R} as the *location* and $[0, 1]$ as the *mark space*. Given parameters $0 < \gamma, \gamma' < 1$, $\beta > 0$, we introduce our notion of connectivity of elements in \mathbb{S} . For $p := (x, u) \in \mathbb{S}$ and $p' := (z, w) \in \mathbb{S}$ we let

$$F(p, p') = F(p, p'; \gamma, \gamma') := |x - z|u^\gamma w^{\gamma'} \quad (2.1)$$

and say that $p \in \mathbb{S}$ and $p' \in \mathbb{S}$ are *connected* if

$$F(p, p'; \gamma, \gamma') \leq \beta. \quad (2.2)$$

We define the *neighborhood* of a point $p \in \mathbb{S}$ by

$$B(p, \beta) = B_F(p, \beta) := \{p' \in \mathbb{S} : F(p, p'; \gamma, \gamma') \leq \beta\}. \quad (2.3)$$

Loosely speaking, we can think of B as a non-metric ball centered at a point $p \in \mathbb{S}$ with radius β . For $\Delta \subseteq \mathbb{S}$, we also put $B_F(\Delta, \beta) := \bigcap_{p \in \Delta} B_F(p, \beta)$ as the joint neighborhood of the points in Δ .

Next we define a random bipartite graph. Let $\mathcal{P}, \mathcal{P}'$ be independent Poisson processes on \mathbb{S} with intensity measures $\lambda|\cdot|, \lambda'|\cdot|$, respectively, where $0 < \lambda, \lambda' < 1$ are fixed parameters and $|\cdot|$ denotes Lebesgue measure on \mathbb{S} . Let $G^{\text{bip}} = G^{\text{bip}}(\mathcal{P}, \mathcal{P}') = G^{\text{bip}}(\mathcal{P}, \mathcal{P}'; \gamma, \gamma', \beta)$ be the bipartite graph with vertex set $\mathcal{P} \cup \mathcal{P}'$, where there is an edge between two points $p \in \mathcal{P}$ and $p' \in \mathcal{P}'$ if and only if p and p' are connected. Note that given \mathcal{P} and \mathcal{P}' , the number of edges in G^{bip} is increasing in the parameters γ, γ' and β and that $\mathcal{P}' \cap B_F(p, \beta)$ is the subset of points in \mathcal{P}' connected to p in G^{bip} .

In the collaboration network example discussed in Section 9 below, the Poisson processes \mathcal{P} and \mathcal{P}' can be thought of as sets of authors and documents, respectively. An edge (p, p') can be interpreted as the relation

that author $p \in \mathcal{P}$ has collaborated on manuscript $p' \in \mathcal{P}'$. Considering the product on the right-hand side of (2.1) illustrates that G^{bip} is a natural bipartite extension of the age-dependent random connection models from [10, 12]. As will be made precise below, $\gamma, \gamma' < 1$ determine the power-law exponent of the degree distribution for vertices in $\mathcal{P}, \mathcal{P}'$, respectively. Once γ, γ' are fixed, the parameter $\beta > 0$ can be used to tune the overall number of expected edges in the bipartite graph G^{bip} .

Note that it follows from identity (2.1) that the roles of \mathcal{P} and \mathcal{P}' are symmetric when switching the parameters γ and γ' . Hence, when in the following we describe more elaborate graph-theoretic and topological quantities of G^{bip} that are defined with reference to \mathcal{P} , the symmetry between \mathcal{P} and \mathcal{P}' implies that our results also hold for the corresponding quantities defined in terms of \mathcal{P}' , when switching the assumptions on γ and γ' .

We now introduce the *random connection hypergraph model (RCHM)* $G^{\text{Dow}} := G^{\text{Dow}}(\mathcal{P}, \mathcal{P}')$ through the construction known as *Dowker complex* [4]. We stress here, that G^{Dow} is a very specific type of hypergraph, namely a simplicial complex. In the following, we rely on this structure as a simplicial to investigate Betti numbers. More precisely, the set of hyperedges Σ_m of G^{Dow} of cardinality $m + 1$ is given by

$$\Sigma_m := \{\Delta_m \subseteq \mathcal{P} : \#(\Delta_m) = m + 1, \mathcal{P}' \cap B_F(\Delta_m, \beta) \neq \emptyset\}, \quad (2.4)$$

where $\#(\cdot)$ denotes the cardinality of a set.

Following the terminology in topological data analysis, we also refer to the elements of Σ_m as *m-simplices*. If there is a unique vertex of an m -simplex Δ_m with a lowest mark, then we define $c(\Delta_m) \in \mathbb{R}$ as the location coordinate of this vertex. Otherwise, let $c(\Delta_m)$ be the location of the left-most vertex among all vertices with minimal mark. Although not explicitly stated, the set of m -simplices Σ_m depends on the point process \mathcal{P}' . In our interpretation, $m + 1$ authors form an m -simplex if and only if they have co-authored at least one common paper.

In classical binary networks, the degree distribution of a typical vertex is of central importance. Due to the translation-invariance of the edge rule (2.2) such a vertex can be chosen to be of the form $o = (0, U)$ with U uniform in $[0, 1]$. For higher-order networks, it is essential to go beyond single vertices and describe properties of typical m -simplices. However, rigorously defining the notion of a typical simplex is far more involved. To address this problem, we will rely on the established theory of Palm calculus as explained in [17]. As a first step, we need to establish that the m -simplex intensity is finite. Given a subset A of \mathbb{R} , we denote the subset of m -simplices centered in A by

$$\Sigma_m^A = \{\Delta_m \in \Sigma_m : c(\Delta_m) \in A\}.$$

Proposition 2.1 (Finiteness of the m -simplex-intensity). *Let \mathcal{P} and \mathcal{P}' be independent Poisson point processes on \mathbb{S} , let $A \subseteq \mathbb{R}$ be a Borel set with Lebesgue measure one. Given $m \geq 0$, $\gamma < 1$, $\gamma' < 1/(m + 1)$ and $\beta > 0$, the m -simplex intensity $\lambda_m := \mathbb{E}[\#\Sigma_m^A]$ is a non-zero finite value not depending on the choice of A .*

Now, we define the distribution of the typical m -simplex Δ_m^* . To do so, we first introduce the following notations. More precisely, f denotes an arbitrary nonnegative measurable functional that may depend on a considered m -simplex as well as on the point processes \mathcal{P} and \mathcal{P}' . Then, we define the distribution of the typical m -simplex as

$$\mathbb{E}[f(\Delta_m^*, \mathcal{P}, \mathcal{P}')] = \frac{1}{\lambda_m} \mathbb{E}\left[\sum_{\Delta_m \in \Sigma_m^A} f(\Delta_m - c(\Delta_m), \mathcal{P} - c(\Delta_m), \mathcal{P}' - c(\Delta_m)) \right] \quad (2.5)$$

where $A \subseteq \mathbb{R}$ is an arbitrary Borel set with $|A| = 1$ and for a set $R \subseteq \mathbb{S}$ and $x \in \mathbb{R}$, we write $R - x := \{(y - x, u) : (y, u) \in R\}$. Note that for translation-invariant f , we can replace $f(\Delta_m - c(\Delta_m), \mathcal{P} - c(\Delta_m), \mathcal{P}' - c(\Delta_m))$ by $f(\Delta_m, \mathcal{P}, \mathcal{P}')$. Note also that if f is bounded, Proposition 2.1 shows that the expectation (2.5) is well-defined.

Now we can derive an integral representation of the Palm distribution. We write $\mathbf{p}_m := (p_1, \dots, p_m)$ for an m -tuple of points, and for $u \in [0, 1]$, we introduce the notations $\mathbf{p}_m(u) := ((0, u), p_1, \dots, p_m)$ and $\overrightarrow{\mathbf{p}_m}(u) := \{(0, u), p_1, \dots, p_m\}$ for the tuple and corresponding set, respectively.

Proposition 2.2 (Distribution of the typical m -simplex). *Let $m \geq 0$, $\gamma < 1$, $\gamma' < 1/(m+1)$, and let f be an arbitrary nonnegative measurable functional depending on an m -simplex as well as on the point processes \mathcal{P} and \mathcal{P}' . Then,*

$$\mathbb{E}[f(\Delta_m^*, \mathcal{P}, \mathcal{P}')] = \frac{\lambda^{m+1}}{\lambda_m(m+1)!} \int_{[0,1] \times \mathbb{S}^m} \mathbb{E}[f(\vec{\mathbf{p}}_m^\rightarrow(u), \mathcal{P} \cup \vec{\mathbf{p}}_m^\rightarrow(u), \mathcal{P}') \mathbb{1}\{\vec{\mathbf{p}}_m^\rightarrow(u) \in \Sigma_m\}] d\mathbf{p}_m du.$$

Here, if $\vec{\mathbf{p}}_m^\rightarrow(u)$ does not consist of precisely $m+1$ elements, then we let $f(\vec{\mathbf{p}}_m^\rightarrow(u), \mathcal{P} \cup \vec{\mathbf{p}}_m^\rightarrow(u), \mathcal{P}') := 0$.

As a first application of the Palm distribution, we show that the higher-order degree distributions are scale-free. In classical binary networks, the degree of a vertex equals the number of edges it is incident to. For instance, in the bipartite graph G^{bip} , the degree of an author-vertex equals the number of papers this author has written. Hence, similarly, for an $(m+1)$ -element subset of authors, we define its higher-order degree as the number of papers this subset has collaborated on. With $\text{Fin}(\mathcal{P})$ denoting the family of finite subsets of \mathcal{P} , we define the bipartite graph with vertex sets $\text{Fin}(\mathcal{P})$ and \mathcal{P}' , and there is an edge between a simplex $\Delta \in \text{Fin}(\mathcal{P})$ and $p' \in \mathcal{P}'$ if and only if $\max_{p \in \Delta} F(p, p'; \gamma, \gamma') \leq \beta$. The degree $\text{deg}(\Delta)$ of a simplex Δ is then the number of points in \mathcal{P}' to which all points in Δ are connected to:

$$\text{deg}(\Delta) := \mathcal{P}'(B_F(\Delta, \beta)) := \#(\mathcal{P}' \cap B_F(\Delta, \beta)).$$

Note that $\text{deg}(\Delta)$ depends in fact on G^{bip} and not only G^{Dow} . In the context of the Dowker complex, $\text{deg}(\Delta)$ can also be interpreted as the number of witnesses for the m -simplex Δ . We now show that the typical higher-order degrees are scale-free in the sense that they satisfy a power law. In particular, for $m=0$, we recover the classical degree distribution of the authors.

Theorem 2.3 (Scale-freeness of higher-order degrees). *Let $m \geq 0$, $\gamma < 1$, $\gamma' < 1/(m+1)$. Then,*

$$\lim_{k \uparrow \infty} \frac{\log \mathbb{P}(\text{deg}(\Delta_m^*) \geq k)}{\log(k)} = m - \frac{m+1}{\gamma}.$$

We note that given a subset σ of \mathcal{P} and a subset τ of \mathcal{P}' , one can say that (σ, τ) forms a biclique in the bipartite graph G^{bip} if every \mathcal{P} -vertex in σ is connected to every \mathcal{P}' -vertex in τ and vice versa. Then, the degree of σ is the number of bicliques of the form (σ, τ) where τ is a set of cardinality exactly one.

From a topological perspective, we note that Theorem 2.3 is loosely related to the multicover bifiltration. Here, considering a union of balls, a point is k -covered if it is contained in the union of at least k of the balls. Similarly, in Theorem 2.3 we have $\text{deg}(\Delta_m^*) \geq k$ if there are at least k points in the set $B_F(\Delta_m, \beta)$.

One of the key advantages of a stochastic network model is that when working with data, we can statistically test the hypothesis whether the model is a good fit for the considered data. To carry out this approach rigorously, we want to use test statistics reflecting key topological properties of the Dowker complex associated with G^{Dow} .

This opens the door towards considering invariants from topological data analysis such as the Betti numbers. Thus, we start by establishing the asymptotic normality of the Betti numbers in the regime $\gamma < 1/4$ in the window $\mathbb{S}_n := [0, n] \times [0, 1]$. To make this precise, fix $m \geq 0$ and let $\beta_m^{(n)}$ denote the m th Betti number of $G^{\text{Dow}}(\mathcal{P} \cap \mathbb{S}_n, \mathcal{P}' \cap \mathbb{S}_n)$. Moreover, let $\mathcal{N}(0, \sigma^2)$ denote the normal distribution with mean 0 and variance σ^2 .

Theorem 2.4 (Asymptotic normality of Betti numbers). *Let $m \geq 0$. Let $\gamma < 1/4$ and $\gamma' < 1/(4(m+1))$. Then, in distribution,*

$$\frac{\beta_m^{(n)} - \mathbb{E}[\beta_m^{(n)}]}{\sqrt{\text{Var}(\beta_m^{(n)})}} \xrightarrow{n \uparrow \infty} \mathcal{N}(0, 1).$$

Note that instead of letting $n \uparrow \infty$, one could alternatively let λ , λ' and β tend to infinity.

Note also that by the Dowker duality theorem [4], $\beta_m^{(n)}$ coincides with the Betti number that is obtained from the dual Dowker complex, where the roles of \mathcal{P} and \mathcal{P}' are reversed.

While the asymptotic normality of test statistics is highly convenient in applied statistics, we stress that Theorem 2.4 requires that $\gamma < 1/4$. Taking into account Theorem 2.3 for $m=0$, we see that this means that the typical degree distribution has a finite fourth moment. However, when considering complex networks, we often encounter the situation where even the variance is infinite. Hence, it is no longer reasonable to expect

a normal distribution in the limit, since the latter exhibits light tails. In analogy to the classical setting of sums of independent heavy-tailed random variables, we expect that the suitably recentered and rescaled distribution converges to a stable distribution.

However, since the Betti numbers are a highly refined topological quantity, giving a rigorous proof of the stable limit convergence in the delicate heavy-tailed setting is difficult. We also note that while there is an ample variety of asymptotically normal test statistics for spatial networks model [13, 20], the stable setting has so far been considered only in selected isolated cases [6].

While establishing a stable limit for the Betti numbers seems to be out of reach for the moment, similarly as in [14], we can prove a stable limit for a much simpler test statistic, namely the edge count

$$S_n := \sum_{P_i \in \mathcal{P} \cap \mathcal{S}_n} \deg(P_i),$$

where we recall that $\deg(P_i)$ denotes the degree of a point P_i in the bipartite graph G^{bip} .

Theorem 2.5 (Normal and stable limits of edge count). *Let $\gamma' < 1/3$. Then, the following distributional limits hold as $n \uparrow \infty$.*

- (a) *Let $\gamma < 1/2$. Then, $n^{-1/2}(S_n - \mathbb{E}[S_n]) \rightarrow \mathcal{N}(0, \sigma^2)$ for some $\sigma \geq 0$.*
- (b) *Let $\gamma \in (1/2, 1)$. Then, $n^{-\gamma}(S_n - \mathbb{E}[S_n]) \rightarrow \mathcal{S}_{\gamma-1}$, where $\mathcal{S}_{\gamma-1}$ is a γ^{-1} -stable random variable.*

While Theorem 2.5 establishes rigorously the desired normal and stable limits in the asserted regimes, it is difficult to apply for hypothesis tests in an actual data analysis. This is because typically the parameter β is tuned such that the expected number of edges in the bipartite model matches the quantity in the data.

Hence, in order to have practically useful test statistics, we now define

$$S_{n,m} := \#\{\Delta_m \in \Sigma_m : c(\Delta_m) \in [0, n]\}$$

as the number of m -simplices centered in $[0, n]$.

The fact that we can extend the proof of Theorem 2.5 to the case of m -simplex count is remarkable. Indeed, in the simpler model considered in [14], this functional seemed out of reach. The explanation is that for the task of proving central and stable limit theorems, our bipartite model is surprisingly more accessible than the one from [14]. The reason is that in the present model, the crucial covariance between simplex counts in disjoint regions become accessible since we can condition on the set \mathcal{P}' and then apply the formula of total covariance. These essential variance- and covariance computations are summarized in the following auxiliary result.

Theorem 2.6 (Normal and stable limits of simplex count). *Let $\gamma' < 1/(2m + 1)$. Then, the following distributional limits hold as $n \uparrow \infty$.*

- (a) *Let $\gamma < 1/2$. Then, $n^{-1/2}(S_{n,m} - \mathbb{E}[S_{n,m}]) \rightarrow \mathcal{N}(0, \sigma^2)$ for some $\sigma \geq 0$.*
- (b) *Let $\gamma \in (1/2, 1)$. Then, $n^{-\gamma}(S_{n,m} - \mathbb{E}[S_{n,m}]) \rightarrow \mathcal{S}_{\gamma-1}$, where $\mathcal{S}_{\gamma-1}$ is an γ^{-1} -stable random variable.*

To relate our model to existing concepts in the literature, we note that there is a standard construction to retrieve a hypergraph from a bipartite graph. This could also be done in our setting with the bipartite graph G^{bip} . After taking closures under subsets, we recover the hypergraph G^{Dow} introduced above.

In the rest of the paper, the parameter β is held fixed. Hence, to ease notation, in the rest of the paper, we write $B_F(\vec{\mathbf{p}}_m)$ instead of $B_F(\vec{\mathbf{p}}_m, \beta)$.

3. PROOF OF PROPOSITIONS 2.1 AND 2.2

Proof of Proposition 2.1. As before, let $A \subseteq \mathbb{R}$ be an arbitrary Borel set with $|A| = 1$. Furthermore, let $g_m(p_0, \dots, p_m, \mathcal{P}')$ denote the indicator of the event that an m -tuple of points forms an m -simplex and that the marks of p_0, \dots, p_m are ordered ascendingly. The m -simplex intensity λ_m is then given by

$$\begin{aligned} \lambda_m &= \mathbb{E} \left[\sum_{\Delta_m \in \Sigma_m} \mathbb{1}\{c(\Delta_m) \in A\} \right] = \lambda^{m+1} \int_{(A \times [0,1]) \times \mathbb{S}^m} \mathbb{E}[g_m((p_0, p_1, \dots, p_m), \mathcal{P}')] \, d(p_0, \mathbf{p}_m) \\ &= \lambda^{m+1} \int_{[0,1] \times \mathbb{S}^m} \mathbb{E}[g_m(\mathbf{p}_m(u), \mathcal{P}')] \, d\mathbf{p}_m \, du, \end{aligned}$$

where we used the Mecke formula [17, Theorem 4.4] in the first step, and integrated with respect to the location of p_0 in the second step. Note that the number of points in the common neighborhood $B(\vec{p}_m(u))$ of the vertices is Poisson-distributed. Hence, by the Markov inequality, the probability that this set is nonempty is given by:

$$\lambda_m = \frac{\lambda^{m+1}}{(m+1)!} \int_0^1 \int_{\mathbb{S}^m} \mathbb{P}(\mathcal{P}'(B(\vec{p}_m(u))) \geq 1) \, d\mathbf{p}_m \, du \leq \frac{\lambda^{m+1} \lambda'}{(m+1)!} \int_0^1 \int_{\mathbb{S}^m} |B(\vec{p}_m(u))| \, d\mathbf{p}_m \, du.$$

The inner integral is given by

$$\int_{\mathbb{S}^m} |B(\vec{p}_m(u))| \, d\mathbf{p}_m = \int_{\mathbb{S}} \mathbf{1}\{|z| \leq \beta u^{-\gamma} w^{-\gamma'}\} \int_{\mathbb{S}^m} \mathbf{1}\{|z - y_i| \leq \beta v_i^{-\gamma} w^{-\gamma'} : 1 \leq i \leq m\} \, d\mathbf{p}_m \, dp'.$$

Next, we integrate with respect to the location coordinates $\mathbf{y} := (y_1, \dots, y_m)$, the marks $\mathbf{v} := (v_1, \dots, v_m)$ as well as z, w, u . This gives for the above

$$\begin{aligned} \int_{\mathbb{S}} \mathbf{1}\{|z| \leq \beta u^{-\gamma} w^{-\gamma'}\} \int_{[0,1]^m} \prod_{i=1}^m (2\beta v_i^{-\gamma} w^{-\gamma'}) \, d\mathbf{v} \, dp' &= \left(\frac{2\beta}{1-\gamma}\right)^m \int_{\mathbb{S}} \mathbf{1}\{|z| \leq \beta u^{-\gamma} w^{-\gamma'}\} w^{-m\gamma'} \, dp' \\ &= \frac{(2\beta)^{m+1}}{(1-\gamma)^m} u^{-\gamma} \int_0^1 w^{-(m+1)\gamma'} \, dw \\ &= \frac{(2\beta)^{m+1}}{(1-\gamma)^m} \frac{u^{-\gamma}}{1-(m+1)\gamma'}, \end{aligned}$$

where we have used that $\gamma < 1$ and $\gamma' < 1/(m+1)$. Using again that $\gamma < 1$, we conclude that $\lambda_m < \infty$. \square

Proof of Proposition 2.2. Let $A \subseteq \mathbb{R}$ be an arbitrary Borel set with $|A| = 1$. Let the lowest-mark \mathcal{P} -vertex $c(\Delta_m)$ of a set of $m+1$ points Δ_m be denoted by $p_0 := (x, u)$. The expectation of a nonnegative functional f is given by (2.5). By another application of the Mecke formula, and by integrating over x , we obtain

$$\mathbb{E}[f(\Delta_m^*, \mathcal{P}, \mathcal{P}')] = \frac{\lambda^{m+1}}{\lambda_m} \int_{[0,1] \times \mathbb{S}^m} \mathbb{E}\left[f(\vec{p}_m(u), \mathcal{P} \cup \vec{p}_m(u), \mathcal{P}') g_m(\mathbf{p}_m(u), \mathcal{P}')\right] \, d\mathbf{p}_m \, du,$$

as asserted. \square

4. PROOF OF THEOREM 2.3

Since the proofs of the upper and lower bounds are very different, we deal with them in Sections 4.1 and 4.2, separately. We start with two lemmas that are used both in the proof of the upper bound.

Lemma 4.1 (Pairwise intersections). *Let $0 \leq u \leq v \leq 1$, and set $o := (0, u) \in \mathbb{S}$ and $p := (y, v) \in \mathbb{S}$. Then, the measure of the intersection of their neighborhood $|B(\{o, p\})|$ can be upper bounded as follows:*

$$|B(\{o, p\})| \leq \frac{2\beta}{1-\gamma'} v^{-\gamma} s_{\wedge}(u, y)^{1-\gamma'} \quad \text{where} \quad s_{\wedge}(u, y) := (2\beta u^{-\gamma} |y|^{-1})^{1/\gamma'} \wedge 1.$$

Proof. For a point $(z, w) \in \mathbb{S}$ to be connected to both $(0, u)$ and (y, v) , it must hold that $|z| \leq \beta u^{-\gamma} w^{-\gamma'}$ and that $|y - z| \leq \beta v^{-\gamma} w^{-\gamma'}$. As $u \leq v$, we find from the triangle inequality that $|y| \leq 2\beta u^{-\gamma} w^{-\gamma'}$ and hence $w \leq (2\beta u^{-\gamma} |y|^{-1})^{1/\gamma'}$. On the other hand, $w \leq 1$, so $w \leq s_{\wedge}(u, y)$ and using only the second condition above for z ,

$$|B(\{o, p\})| \leq \int_0^{s_{\wedge}(u, y)} \int_{-\beta v^{-\gamma} w^{-\gamma'}}^{\beta v^{-\gamma} w^{-\gamma'}} \, dz \, dw = \int_0^{s_{\wedge}(u, y)} 2\beta v^{-\gamma} w^{-\gamma'} \, dw = \frac{2\beta}{1-\gamma'} v^{-\gamma} s_{\wedge}(u, y)^{1-\gamma'},$$

as asserted. \square

Lemma 4.2 (Upper bound of $\int F(s_{\wedge}(u, y)) \, dy$). *Let $\rho > \gamma'$ and $F : (0, \infty) \rightarrow [0, 1]$ be an integrable function. Assume that $c := \sup_{x>0} x^{-\rho} F(x) < \infty$. Then, for all $a \geq 0$,*

$$\int_{-\infty}^{\infty} F(s_{\wedge}(u, y)) \, dy \leq 2a + \frac{2c\gamma'}{\rho - \gamma'} (2\beta)^{\rho/\gamma'} a^{1-\rho/\gamma'} u^{-\rho\gamma'/\gamma'}.$$

Proof. We use the upper bounds of F and the symmetry of $|y|$ to write

$$\begin{aligned} \int_{-\infty}^{\infty} F(s_{\wedge}(u, y)) \, dy &\leq 2 \int_0^a 1 \, dy + 2c \int_a^{\infty} s_{\wedge}(u, y)^{\rho} \, dy \leq 2a + 2c (2\beta u^{-\gamma})^{\rho/\gamma'} \int_a^{\infty} y^{-\rho/\gamma'} \, dy \\ &\leq 2a + \frac{2c\gamma'}{\rho - \gamma'} (2\beta)^{\rho/\gamma'} a^{1-\rho/\gamma'} u^{-\rho/\gamma'}, \end{aligned}$$

where we have used that $\rho > \gamma'$. □

4.1. Proof of Theorem 2.3 – upper bound. The key idea for the proof of the upper bound is to note that if all points of Δ_m have a common neighbor in \mathcal{P}' , then also all pairs of \mathcal{P} -vertices in Δ_m have a common neighbor. This observation will be used to subsequently bound the integrals in the Palm probabilities.

Proof of the upper bound. By Proposition 2.2 we obtain that

$$\mathbb{P}(\deg(\Delta_m^*) \geq k) = \frac{\lambda^{m+1}}{\lambda_m(m+1)!} \int_{[0,1]} \int_{\mathbb{S}^m} \mathbb{P}(\mathcal{P}'(B(\vec{\mathbf{p}}_m(u))) \geq k) \, d\mathbf{p}_m \, du.$$

Let $b := \lambda' |B(\vec{\mathbf{p}}_m(u))|$ and note that $X := \mathcal{P}'(B(\vec{\mathbf{p}}_m(u)))$ is Poisson-distributed with parameter b . Next, we upper bound the probability by distinguishing whether $b_{\cap} \geq k/2$ or not,

$$\mathbb{P}(X \geq k) \leq \mathbb{1}\{b \geq k/2\} + \mathbb{P}(X \geq k) \mathbb{1}\{b < k/2\}.$$

Our goal is to show that the second term is negligible compared to the first for large k . First,

$$\mathbb{P}(X \geq k) = \mathbb{P}(X \geq 1) \frac{\mathbb{P}(X \geq k)}{\mathbb{P}(X \geq 1)}.$$

Let $b_{\vee} := 2 \vee e^2 b$. The numerator is upper bounded by $(b/k)^{k/2}$ whenever $k \geq b_{\vee}$ using [18, Lemma 1.2]. If $b < 1/2$, the denominator can be bounded from below by $1 - \exp(-b) \geq b/2$. Otherwise, the denominator can be bounded from below by a finite constant $1/c_2$. Thus, for $k \geq b_{\vee}$, we have

$$\frac{\mathbb{P}(X \geq k)}{\mathbb{P}(X \geq 1)} \leq c_1 \left(\frac{b}{k}\right)^{k/2} \left(\frac{2}{b} \mathbb{1}\{b < 1/2\} + c_2 \mathbb{1}\{b \geq 1/2\}\right) \leq c_3 (b/k)^{k/2-1}$$

for some $c_1, c_2, c_3 > 0$. Considering the indicator $\mathbb{1}\{b < k/2\}$ in the integrand, we can conclude that

$$\int_{[0,1] \times \mathbb{S}^m} \mathbb{P}(X \geq k) \mathbb{1}\{b < \frac{k}{2}\} \, du \, d\mathbf{p}_m \leq c_3 2^{1-\frac{k}{2}} \int_{[0,1] \times \mathbb{S}^m} \mathbb{P}(X \geq 1) \, du \, d\mathbf{p}_m = c_4 2^{-\frac{k}{2}},$$

where $c_4 > 0$ and in the last step we used that the integral above is finite due to Proposition 2.1. As shown below, the $\mathbb{1}\{b \geq k/2\}$ term decays as a power law with increasing k . Thus,

$$\limsup_{k \uparrow \infty} \frac{\log \mathbb{P}(\deg(\Delta_m^*) \geq k)}{\log k} \leq \limsup_{k \uparrow \infty} \frac{\log \int_{[0,1] \times \mathbb{S}^m} \mathbb{1}\{b \geq k/2\} \, d(u, \mathbf{p}_m)}{\log k}.$$

In particular, for $m = 0$

$$\begin{aligned} \int_{[0,1]} \mathbb{1}\{b \geq k/2\} \, du &= \int_{[0,1]} \mathbb{1}\left\{\lambda' \int_{\mathbb{R} \times [0,1]} \mathbb{1}\{|z| \leq \beta u^{-\gamma} w^{-\gamma'}\} \, dz \, dw \geq k/2\right\} \, du \\ &= \int_{[0,1]} \mathbb{1}\left\{\frac{2\beta\lambda'}{1-\gamma'} u^{-\gamma} \geq k/2\right\} \, du \in O(k^{-1/\gamma}), \end{aligned}$$

This concludes the proof for $m = 0$.

From now on we assume $m \geq 1$. Our goal is to upper bound the expression

$$\limsup_{k \uparrow \infty} \frac{\log \mathbb{P}(\deg(\Delta_m^*) \geq k)}{\log(k)} \leq \limsup_{k \uparrow \infty} \left(\frac{1}{\log(k)} \log \left(\int_{[0,1] \times \mathbb{S}^m} \mathbb{1}\{b \geq k/2\} \, du \, d\mathbf{p} \right) \right).$$

From now on, we assume that the points p_i are ordered in increasing order of their marks, i.e., $u \leq v_1 \leq \dots \leq v_m$. Note that

$$b \leq \lambda' |B(\vec{\mathbf{p}}_1(u))| \wedge \min_{i=1, \dots, m-1} \lambda' |B(\{p_i, p_{i+1}\})|.$$

Due to translation invariance and Lemma 4.1 we find that for some constant $c > 0$,

$$\lambda' |B(\{p_i, p_{i+1}\})| = \lambda' |B(\{(0, v_i), (y_{i+1} - y_i, v_{i+1})\})| \leq c v_{i+1}^{-\gamma} s_\wedge(v_i, y_{i+1} - y_i)^{1-\gamma'}.$$

Using this upper bound,

$$\int_{[0,1] \times \mathbb{S}^m} \mathbb{1}\{b \geq k/2\} d(u, \mathbf{p}_m) \leq \int_{[0,1] \times \mathbb{S}^m} \prod_{i=0}^{m-1} \mathbb{1}\{c v_{i+1}^{-\gamma} s_\wedge(v_i, y_{i+1} - y_i)^{1-\gamma'} \geq k\} d(u, \mathbf{p}_m),$$

where we have set $v_0 := u$ and $y_0 := 0$. In the indicators, we can express the upper limit of the marks v_i ,

$$\int_0^{ck^{-1/\gamma}} \int_{\mathbb{S}^m} \prod_{i=0}^{m-1} \mathbb{1}\{v_{i+1} \leq c s_\wedge(v_i, y_{i+1} - y_i)^{(1-\gamma')/\gamma} k^{-1/\gamma}\} d\mathbf{p}_m du,$$

where we set the upper limit of the integral with respect to u to $ck^{-1/\gamma}$ as $u \leq v_1 \leq ck^{-1/\gamma}$. We now substitute $y'_{i+1} := y_{i+1} - y_i$ for $i = 0, \dots, m-1$. Furthermore, let $p'_i := (y'_i, v_i)$ denote the i th point with the new coordinates. Then we have

$$\int_0^{ck^{-1/\gamma}} \int_{\mathbb{S}^m} \prod_{i=0}^{m-1} \mathbb{1}\{v_{i+1} \leq c s_\wedge(v_i, y'_{i+1})^{(1-\gamma')/\gamma} k^{-1/\gamma}\} d\mathbf{p}'_m du.$$

Note that the point $p'_m = (y'_m, v_m)$ only appears in one of the indicators in the product. We integrate this indicator with respect to p'_m . Then, for large k ,

$$\int_{\mathbb{R} \times [0,1]} \mathbb{1}\{v_m \leq c s_\wedge(v_{m-1}, y'_m)^{(1-\gamma')/\gamma} k^{-1/\gamma}\} dp'_m = \int_{\mathbb{R}} ck^{-1/\gamma} s_\wedge(v_{m-1}, y'_m)^{(1-\gamma')/\gamma} dy'_m \in O(k^{-1/\gamma} v_{m-1}^{-\gamma}),$$

where in the first step we noted that the indicator represents an upper bound of v_m and integrated it out, and in the second step we used Lemma 4.2 with $\rho = (1 - \gamma')/\gamma$ and $a = u^{-\gamma}$. Note that the finiteness of integral requires that $\gamma < (1 - \gamma')/\gamma'$. We can follow the same steps for integrating out with respect to p'_{m-1} . The only difference is that now a $v_{m-1}^{-\gamma}$ appears in the integration, resulting in a $k^{(1-\gamma)/\gamma}$ factor. Then,

$$\begin{aligned} \int_{[0,1] \times \mathbb{S}^m} \mathbb{1}\{b \geq k/2\} d(u, \mathbf{p}_m) &\leq ck^{-(1+(m-2)(1-\gamma))/\gamma} \int_0^{ck^{-1/\gamma}} \int_{\mathbb{R} \times [0,1]} \mathbb{1}\{c v_1^{-\gamma} s_\wedge(u, y'_1)^{1-\gamma'} \geq k\} v_1^{-\gamma} dp'_1 du \\ &\leq ck^{-(1+(m-1)(1-\gamma))/\gamma} \int_0^{ck^{-1/\gamma}} u^{-\gamma} du \in O(k^{m-(m+1)/\gamma}). \end{aligned}$$

This leads to

$$\lim_{k \uparrow \infty} \left(\frac{1}{\log(k)} \log \left(\int_{[0,1] \times \mathbb{S}^m} \mathbb{1}\{b \geq k/2\} d(u, \mathbf{p}_m) \right) \right) = m - \frac{m+1}{\gamma},$$

as asserted. \square

4.2. Proof of Theorem 2.3 – lower bound. The idea for the proof of the lower bound is to construct specific configurations leading to higher-order degrees exceeding. Then, we show that these configurations occur with a sufficiently high probability.

Proof of the lower bound. Let $R_k := [0, k] \times [0, (\beta/k)^{1/\gamma}] \subseteq \mathbb{S}$ and note that for $p := (y, v) \in R_k$ and $p' := (z, w) \in [0, k] \times [0, 1]$, p and p' are connected. Indeed, $|y - z| \leq k \leq \beta u^{-\gamma} w^{-\gamma'}$. This gives for $\nu(k) := \lambda'k - \log(2)$ by Proposition 2.2,

$$\begin{aligned} \mathbb{P}(\deg(\Delta_m^*) \geq \nu(k)) &\geq \frac{\lambda^{m+1}}{\lambda_m(m+1)!} \int_{R_k^m} \int_{[0, (\beta/k)^{1/\gamma}]} \mathbb{P}(\deg(\vec{\mathbf{p}}_m(u)) \geq \nu(k)) du d\mathbf{p}_m \\ &\geq \frac{\lambda^{m+1}(\beta/k)^{1/\gamma}}{\lambda_m(m+1)!} \int_{R_k^m} \mathbb{P}(\mathcal{P}'([0, k] \times [0, 1]) \geq \nu(k)) d\mathbf{p}_m, \end{aligned}$$

As $\mathcal{P}'([0, k] \times [0, 1]) \sim \text{Poi}(\lambda'k)$, its median can be lower bounded by $\nu(k)$ [5, Theorem 2]. Thus, lower bounding the integrand, we obtain

$$\mathbb{P}(\deg(\Delta_m^*) \geq \nu(k)) \geq \frac{\lambda^{m+1}(\beta/k)^{1/\gamma}}{2\lambda_m(m+1)!} |R_k|^m = \frac{\lambda^{m+1}\beta^{(m+1)/\gamma}}{2\lambda_m(m+1)!} k^{m-(m+1)/\gamma}.$$

Hence,

$$\liminf_{k \uparrow \infty} \frac{\log \left(\mathbb{P}(\deg(\Delta_m^*) \geq k) \right)}{\log(k)} = \liminf_{k \uparrow \infty} \frac{\log \left(\mathbb{P}(\deg(\Delta_m^*) \geq \nu(k)) \right)}{\log(k)} \geq m - \frac{m+1}{\gamma},$$

as asserted. \square

5. PROOF OF THEOREM 2.4

The proof of the CLT for the Betti numbers relies on the general Poisson CLT from [20, Theorem 3.1]. This result requires the verification of two conditions, namely a stabilization and a moment condition.

The stabilization condition follows from an adaptation of the arguments provided in [13, 14]. However, the moment condition is more involved than in [13, 14]. This is because in contrast to [13, 14], the existence of an m -simplex can no longer be determined just from the knowledge of the positions of the $m+1$ \mathcal{P} -vertices. Indeed, the existence fundamentally involves the second Poisson process \mathcal{P}' .

Let $\beta(\mathcal{P}, \mathcal{P}') := \beta_{n,m}(\mathcal{P}, \mathcal{P}')$ be the m th Betti number of $G_n^{\text{Dow}}(\mathcal{P} \cap \mathbb{S}_n, \mathcal{P}' \cap \mathbb{S}_n)$. We introduce the two special points $o := (0, U)$, $o' := (0, W)$. Furthermore, let $G_{n,o}^{\text{Dow}} := G^{\text{Dow}}((\mathcal{P} \cup \{o\}) \cap \mathbb{S}_n, \mathcal{P}' \cap \mathbb{S}_n)$ denote the hypergraph in the window \mathbb{S}_n with the additional \mathcal{P} -vertex o , and similarly, let $G_{n,o'}^{\text{Dow}}(\mathcal{P} \cap \mathbb{S}_n, (\mathcal{P}' \cup \{o'\}) \cap \mathbb{S}_n)$ denote the hypergraph in the window \mathbb{S}_n with the additional \mathcal{P}' -vertex o' . Using these notations, the add-one cost operators

$$\begin{aligned} \delta(G_n^{\text{Dow}}, o) &:= \beta(G_{n,o}^{\text{Dow}}) - \beta(G_n^{\text{Dow}}) \\ \delta(G_n^{\text{Dow}}, o') &:= \beta(G_{n,o'}^{\text{Dow}}) - \beta(G_n^{\text{Dow}}). \end{aligned}$$

To apply [20, Theorem 3.1], we need to verify the following conditions:

- a. **moment condition:** $\sup_{n \geq 1} \mathbb{E}[\delta(G_n^{\text{Dow}}, o)^4] < \infty$ and $\sup_{n \geq 1} \mathbb{E}[\delta(G_n^{\text{Dow}}, o')^4] < \infty$.
- b. **weak stabilization:** $\lim_{n \uparrow \infty} \delta(G_n^{\text{Dow}}, o) < \infty$ and $\lim_{n \uparrow \infty} \delta(G_n^{\text{Dow}}, o') < \infty$.

Proof of moment condition. By [13, Lemma 2.9] [8, Chapter VII], $\delta(G_n^{\text{Dow}}, o)$ and $\delta(G_n^{\text{Dow}}, o')$ are bounded above by the number of m - and $(m+1)$ -simplices containing the additional \mathcal{P} -vertex $o = (0, U) \in \mathcal{P}$ or $o' = (0, W) \in \mathcal{P}'$.

We first consider the case of $\delta(G_n^{\text{Dow}}, o')$. The number of new $m-1$ -simplices is given as the number of m -tuples of points in the neighborhood $B(o')$ of the new point $(0, W) \in \mathcal{P}'$:

$$\mathbb{E}[\delta(G_n^{\text{Dow}}, o')^4] \leq \mathbb{E} \left[\binom{\mathcal{P}(B(o'))}{m}^4 \right] \leq \mathbb{E}[\mathcal{P}(B(o'))^{4m}].$$

The number of points in the neighborhood $\mathcal{P}(B(o'))$ is Poisson distributed with mean $\lambda|B(o')| = (2\beta\lambda)/(1-\gamma)w^{-\gamma'}$, as shown in Proposition 2.1. Now, we note since the r th factorial moment of a Poisson random variable with parameter $\mu > 0$ equals μ^r , the r th moment itself is bounded above by $c_{M,r}\mu^r$ for some constant $c_{M,4m} > 0$. Now, noting that $\gamma' < 1/(4m)$, we conclude that

$$\mathbb{E}[\mathcal{P}(B(o'))^{4m}] \leq c_{M,4m} \mathbb{E} \left[\left(\frac{2\beta}{1-\gamma} W^{-\gamma'} \right)^{4m} \right] \leq c \int_0^1 w^{-4m\gamma'} dw < \infty$$

for some $c > 0$.

Next, we show that $\mathbb{E}[\delta(G_n^{\text{Dow}}, o)^4] < \infty$. The number of new m -simplices are formed by the sets of m points $\vec{p}_m := \{p_1, \dots, p_m\} \subseteq \mathcal{P}$ for which a common neighbor $p' \in \mathcal{P}'$ exists with the new \mathcal{P} -vertex o . As this number upper bounds $\delta(G_n^{\text{Dow}}, o)$, we have

$$\mathbb{E}[\delta(G_n^{\text{Dow}}, o)^4] \leq \mathbb{E} \left[\left(\sum_{\mathbf{p}_m \in \mathcal{P}_m^{\neq}} \mathbb{1} \{ \mathcal{P}'(B(\{o\} \cup \vec{p}_m)) \geq 1 \} \right)^4 \right] \leq \mathbb{E} \left[\left(\sum_{p' \in \mathcal{P}'} \binom{\mathcal{P}(B(p'))}{m} \mathbb{1} \{ p' \in B(o) \} \right)^4 \right],$$

where $\vec{p}_m' := \{p'_1, \dots, p'_m\}$, and in the second step each term of the sum represents the number of m -tuples of \mathcal{P} -vertices in the neighborhood of a point $p' \in \mathcal{P}'$, and the indicator ensures that this point is in turn

connected to the new \mathcal{P} -vertex o . We bound the binomial coefficient by $\mathcal{P}(B(p'))^m$, and expand the fourth power of the sum by using the multinomial theorem to obtain

$$\begin{aligned}
\mathbb{E}[\delta(G_n^{\text{Dow}}, o)^4] &\leq c_1 \mathbb{E} \left[\sum_{\mathbf{p}'_4 \in \mathcal{P}'^4} \prod_{i \leq 4} \mathcal{P}(B(p'_i))^m \mathbb{1}\{\vec{\mathbf{p}}'_4 \subseteq B(o)\} \right] && \text{--- term I} \\
&+ c_2 \mathbb{E} \left[\sum_{\mathbf{p}'_3 \in \mathcal{P}'^3} \mathcal{P}(B(p'_1))^{2m} \prod_{i=2}^3 \mathcal{P}(B(p'_i))^m \mathbb{1}\{\vec{\mathbf{p}}'_3 \subseteq B(o)\} \right] && \text{--- term II} \\
&+ c_3 \mathbb{E} \left[\sum_{\mathbf{p}'_2 \in \mathcal{P}'^2} \mathcal{P}(B(p'_1))^{2m} \mathcal{P}(B(p'_2))^{2m} \mathbb{1}\{\vec{\mathbf{p}}'_2 \subseteq B(o)\} \right] && \text{--- term III} \\
&+ c_4 \mathbb{E} \left[\sum_{\mathbf{p}'_2 \in \mathcal{P}'^2} \mathcal{P}(B(p'_1))^{3m} \mathcal{P}(B(p'_2))^m \mathbb{1}\{\vec{\mathbf{p}}'_2 \subseteq B(o)\} \right] && \text{--- term IV} \\
&+ c_5 \mathbb{E} \left[\sum_{p' \in \mathcal{P}'} \mathcal{P}(B(p'))^{4m} \mathbb{1}\{p' \in B(o)\} \right] && \text{--- term V}
\end{aligned}$$

for some $c_1, \dots, c_5 > 0$. To show the moment bound, it is enough to show that each of the above terms is finite. We begin with using the multivariate Mecke formula for term I:

$$I := c_1 \mathbb{E} \left[\sum_{\mathbf{p}'_4 \in \mathcal{P}'^4} \prod_{i \leq 4} \mathcal{P}(B(p'_i))^m \mathbb{1}\{\vec{\mathbf{p}}'_4 \subseteq B(o)\} \right] = c_1 \iint_{[0,1] \times \mathbb{S}^4} \mathbb{E} \left[\prod_{i \leq 4} \mathcal{P}(B(p'_i))^m \mathbb{1}\{p'_i \in B(o)\} \right] du d\mathbf{p}'_4.$$

Introducing the notation $p'_i := (z_i, w_i)$ for the coordinates of the points p'_i , the indicator represents an upper bound for the coordinates $|z_i| \leq \beta u^{-\gamma} w_i^{-\gamma'}$. Next, we use Hölder's inequality to upper bound the expectation of the product:

$$I \leq 2^4 c_1 \iint_{[0,1] \times [0,1]^4} \prod_{i \leq 4} \left(\int_0^{\beta u^{-\gamma} w_i^{-\gamma'}} \mathbb{E} \left[\mathcal{P}(B((z_i, w_i)))^{4m\gamma} \right]^{1/4} dz_i \right) du d\mathbf{w}.$$

Hence,

$$I \leq 2^4 c_1 \iint_{[0,1] \times [0,1]^4} \prod_{i \leq 4} \left(\int_0^{\beta u^{-\gamma} w_i^{-\gamma'}} c_{\mathcal{M}, 4m} \left(\frac{2\beta}{1-\gamma} w_i^{-\gamma'} \right)^m dz_i \right) du d\mathbf{w}.$$

Note that the upper bound does not depend on the variable z_i , as it is translation invariant. Also, we can upper bound the exponential term by a sufficiently large constant C to get

$$I \leq \left(\frac{C(2\beta)^{(m+1)}}{(1-\gamma)^m} \right)^4 c_1 \int_0^1 u^{-4\gamma} du \int_{[0,1]^4} \prod_{i=1}^4 w_i^{-(m+1)\gamma'} d\mathbf{w}.$$

The integral over the w_i is finite whenever $\gamma' < 1/(m+1)$, and the integral over u is finite if $\gamma < 1/4$. The other terms can be bounded similarly, and we obtain a finite bound for $\mathbb{E}[\delta(G_n^{\text{Dow}}, o)^4]$. The conditions for the finiteness of the integrals are given as follows:

- term I: $\gamma < 1/4$ and $\gamma' < 1/(m+1)$,
- term II: $\gamma < 1/3$ and $\gamma' < 1/(2m+1)$,
- term III: $\gamma < 1/2$ and $\gamma' < 1/(2m+1)$,
- term IV: $\gamma < 1/2$ and $\gamma' < 1/(3m+1)$,
- term V: $\gamma < 1$ and $\gamma' < 1/(4m+1)$.

Combining these conditions, we obtain that $\gamma < 1/4$ and $\gamma' < 1/(4m+1)$ are sufficient conditions for the finiteness of $\mathbb{E}[\delta(G_n^{\text{Dow}}, o)^4]$. \square

Proof of weak stabilization. In the following, we extend the arguments from [13, Proposition 5.4].

For $n \geq 1$ we write

$$\beta_n := \dim(Z_n) - \dim(B_n) := \dim(Z(G_n^{\text{Dow}})) - \dim(B(G_n^{\text{Dow}}))$$

for the Betti number of G_n^{Dow} , where Z_n is the corresponding cycle space and B_n is the boundary space.

We set for $o := (0, U)$,

$$\beta_{n,o} := \dim(Z_{n,o}) - \dim(B_{n,o}) := \dim(Z(G_{n,o}^{\text{Dow}})) - \dim(B(G_{n,o}^{\text{Dow}})).$$

Hence, it suffices to prove the weak stabilization with respect to $\dim(Z_n)$ and $\dim(B_n)$ separately. Since the arguments are very similar, we henceforth only deal with the case $\dim(Z_n)$. We do this by showing that $\dim(Z_{n,o}) - \dim(Z_n)$ is non-decreasing and bounded in n .

For the boundedness, note that $\dim(Z_{n,o}) - \dim(Z_n) \leq \deg_{m,n}(o)$, where $\deg_{m,n}(o)$ is the number of m -simplices in \mathbb{S}_n containing the typical \mathcal{P} -vertex o . This is because the m -simplices constructed from $G_{n,o}^{\text{Dow}}$ can be decomposed into the set of m -simplices containing o and into the family of all m -simplices formed in G_n^{Dow} (see [13, Lemma 2.9] for details). To show that $\dim(Z_{n,o}) - \dim(Z_n)$ is non-decreasing, take $n_1 \leq n_2$, and consider the canonical map

$$Z_{n_1,o} \rightarrow Z_{n_2,o}/Z_{n_2}$$

with kernel $Z_{n_1,o'} \cap Z_{n_2} \subseteq Z_{n_1}$. We claim that the kernel is equal to Z_{n_1} . Let M_n and $M_{n,o}$ denote the set of m -simplices in G_n^{Dow} and $G_{n,o}^{\text{Dow}}$, respectively, and consider an m -simplex $\sigma \in M_{n_1,o} \cap M_{n_2}$ forming an m -cycle z . If $\sigma \in M_{n_1}$, then both $\sigma \in M_{n_1,o}$ and $\sigma \in M_{n_2}$. Therefore, $Z_{n_1,o'} \cap Z_{n_2} \subseteq Z_{n_1}$. This means that the induced map

$$Z_{n_1,o}/Z_{n_1} \rightarrow Z_{n_2,o}/Z_{n_2}$$

is injective. In particular, $\dim(Z_{n_1,o}) - \dim(Z_{n_1}) \leq \dim(Z_{n_2,o}) - \dim(Z_{n_2})$, which shows the assertion.

Now, we show the weak stabilization with respect to the typical \mathcal{P}' -vertex $o' \in \mathcal{P}'$. As before, we write

$$\beta'_n := \dim(Z_{n,o'}) - \dim(B_{n,o'}) := \dim(Z(G_{n,o'}^{\text{Dow}})) - \dim(B(G_{n,o'}^{\text{Dow}})),$$

and prove weak stabilization with respect to $\dim(Z_n)$.

Let M_n and $M_{n,o'}$ denote the set of m -simplices in G_n^{Dow} and $G_{n,o'}^{\text{Dow}}$, respectively. Following the same arguments as above, the difference $\dim(Z_{n,o'}) - \dim(Z_n)$ is bounded from above by the number of m -simplices $|M_{n,o'}| - |M_n|$ appearing in G_n^{Dow} due to the addition of the typical \mathcal{P}' -vertex o' :

$$\dim(Z_{n,o'}) - \dim(Z_n) \leq |M_{n,o'}| - |M_n|.$$

In turn, $|M_{n,o'}| - |M_n|$ is bounded from above by the number of m -tuples of points $p \in \mathcal{P}$ in the neighborhood $\mathcal{P}(B(o'))$ of o' :

$$\dim(Z_{n,o'}) - \dim(Z_n) \leq \binom{\mathcal{P}(B(o'))}{m} < \infty,$$

since the neighborhood $\mathcal{P}(B(o'))$ is almost surely finite.

We consider again the canonical map

$$Z_{n_1,o'} \rightarrow Z_{n_2,o'}/Z_{n_2},$$

where $n_1 \leq n_2$. As $Z_{n_1} \subseteq Z_{n_2}$, the kernel of the map is $Z_{n_1,o'} \cap Z_{n_2}$. If $Z_{n_1} = Z_{n_1,o'} \cap Z_{n_2}$, we can conclude the proof as above.

In contrast to the case above, however, $\dim(Z_{n,o'}) - \dim(Z_n)$ is not necessarily monotone, since $Z_{n_1,o'} \cap Z_{n_2} \neq Z_{n_1}$, i.e., there can be cycles in the kernel that are not in Z_{n_1} . To see this, consider a cycle $z \in Z_{n_1,o'} \setminus Z_{n_1}$. If z contains a simplex formed by a \mathcal{P}' -vertex in the increased window size n_2 , but not in the window size n_1 , then $z \in Z_{n_2} \setminus Z_{n_1}$. Thus, $z \notin Z_{n_1}$, but is in the kernel of the map $Z_{n_1,o'} \rightarrow Z_{n_2,o'}/Z_{n_2}$. To solve this problem, we construct a random N_2 such that for any two window sizes $n_2 \geq n_1 \geq N_2$ we have $Z_{n_1,o'} \cap Z_{n_2} = Z_{n_1}$ in the kernel of the map $Z_{n_1,o'} \rightarrow Z_{n_2,o'}/Z_{n_2}$ the sequence $(\dim(Z_{n,o'}) - \dim(Z_n))$ is monotone. Once we have shown this, we can conclude the proof as above.

To construct N_2 , first observe that as $\mathcal{P}(B(o'))$ is almost surely finite, there a random $N_1 \geq 1$ such that for all $n \geq N_1$, the number of m -simplices $|M_{n,o'}| - |M_n|$ is a non-increasing sequence. As all \mathcal{P} -vertices in the neighborhood $B(o')$ have finite neighborhoods almost surely, there also exists $N_2 \geq N_1 \in \mathbb{R}$ such that for all $n \geq N_2$, the number of m -simplices $|M_{n,o'}| - |M_n|$ is a non-decreasing sequence, and thus constant for such n . Then, we conclude the proof as above. \square

6. PROOF OF THEOREM 2.5

The proof idea for Theorem 2.5 is similar to the edge-count CLTs and stable limits obtained in [14]. For the CLT, we use a general result on associated random variables, whereas for the stable case, we use a truncation argument and a comparison with the independent case. Besides some moment computations of the degree of a typical node, the main difficulty in the proof is to approximate the random number of nodes in the interval $[0, n]$ by a deterministic number.

We begin by proving an auxiliary result that will be used both in the normal and the stable case. Recall the definition of the neighborhood $B(\Delta)$ of a set of points Δ as it was defined in (2.3). As before, for $u \leq 1$ and $\vec{p}_m \subseteq \mathcal{P}$, we write $B(\vec{p}_m)(u)$ for the common neighborhood of $\{(0, u), p_1, \dots, p_m\}$.

Lemma 6.1 (Scaling of $B(\vec{\mathbf{p}}_m(u))$). *Let $u \leq 1$, $m \geq 1$, $0 < \gamma < 1$ and $0 < \gamma' < 1/(m+1)$. It holds that*

$$\int_{\mathbb{S}^m} |B(\vec{\mathbf{p}}_m(u))| d\mathbf{p}_m = \frac{u^{-\gamma}}{1 - (m+1)\gamma'} \frac{(2\beta)^{m+1}}{(1-\gamma)^m}.$$

Proof. We have that

$$\begin{aligned} \int_{\mathbb{S}^m} |B(\vec{\mathbf{p}}_m(u))| d\mathbf{p}_m &= \iint_{\mathbb{S} \times \mathbb{S}^m} \mathbb{1}\{p' \in B(\vec{\mathbf{p}}_m(u))\} d\mathbf{p}_m dp' \\ &= \int_{\mathbb{S}} \mathbb{1}\{(z, w) \in B(o)\} \left(\int_{\mathbb{S}} \mathbb{1}\{|z-y| \leq \beta v^{-\gamma} w^{-\gamma'}\} d(y, v) \right)^m d(z, w) \\ &= \int_{\mathbb{S}} \mathbb{1}\{(z, w) \in B(o)\} \left(\frac{2\beta w^{-\gamma'}}{1-\gamma} \right)^m d(z, w) \\ &= u^{-\gamma} \int_0^1 \frac{(2\beta w^{-\gamma'})^{m+1}}{(1-\gamma)^m} dw = \frac{u^{-\gamma}}{1 - (m+1)\gamma'} \frac{(2\beta)^{m+1}}{(1-\gamma)^m}, \end{aligned}$$

where we used the notations $p := (y, v)$ and $p' := (z, w)$. \square

6.1. Proof of Theorem 2.5– normal limit. The idea of the proof is to apply the central limit theorem [27, Theorem 4.4.3] which holds for stationary sequences of identically distributed associated random variables $\mathbf{T} := T_1, T_2, \dots$, and requires that $\sum_{k \geq 1} \text{Cov}(T_1, T_k) < \infty$. Recall that the sequence of random variables \mathbf{T} is associated if and only if $\text{Cov}(f(T_1, \dots, T_k), g(T_1, \dots, T_k)) \geq 0$ for all non-decreasing functions f, g for which $\mathbb{E}[f(T_1, \dots, T_k)], \mathbb{E}[g(T_1, \dots, T_k)], \mathbb{E}[f(T_1, \dots, T_k)g(T_1, \dots, T_k)]$ exist [9, Definition 1.1].

Proof of Theorem 2.5(a). Let $\gamma < 1/2$ and define for $i \geq 1$,

$$T_i := \sum_{P_j \in [i-1, i] \times [0, 1]} \deg(P_j).$$

Since the degree $\deg(x, u)$ is increasing in the Poisson process \mathcal{P}' , we conclude from the Harris-FKG inequality [17, Theorem 20.4] that the sequence T_1, \dots, T_k is associated. For $A \subseteq \mathbb{R}$ let

$$S(A) := \sum_{P_j \in \mathcal{P} \cap A \times [0, 1]} \deg(P_j).$$

Then, the Mecke equation gives

$$\begin{aligned} \text{Var}(S(A)) &= \mathbb{E} \left[\sum_{P_i \neq P_j \in \mathcal{P} \cap A} \deg(P_i) \deg(P_j) \right] + \mathbb{E} \left[\sum_{P_i \in \mathcal{P} \cap A} \deg(P_i)^2 \right] - \mathbb{E} \left[\sum_{P_i \in \mathcal{P} \cap A} \deg(P_i) \right]^2 \\ &= \lambda^2 \iint_{(A \times [0, 1])^2} \mathbb{E}[\deg(x, u) \deg(y, v)] d(x, u) d(y, v) \\ &\quad + \lambda \int_{A \times [0, 1]} \mathbb{E}[\deg(x, u)^2] d(x, u) - \lambda^2 \left(\int_{A \times [0, 1]} \mathbb{E}[\deg(x, u)] d(x, u) \right)^2 \\ &= \lambda |A| \int_0^1 \mathbb{E}[\deg(0, u)^2] du + \lambda^2 \iint_{A \times [0, 1]} \text{Cov}(\deg(x, u), \deg(y, v)) d(x, u) d(y, v), \end{aligned}$$

where the last equality holds due to translation invariance of $\deg(\cdot)$.

To bound the first integral, note that for all $u \in [0, 1]$, the random variable $\deg(0, u)$ is Poisson distributed with parameter $\frac{2\beta}{1-\gamma'} u^{-\gamma}$. Hence, $\mathbb{E}[\deg(0, u)^2] = \frac{2\beta}{1-\gamma'} u^{-\gamma} (1 + \frac{2\beta}{1-\gamma'} u^{-\gamma}) \in O(u^{-2\gamma})$. Thus, we obtain for $\gamma < 1/2$ that $\int_0^1 \mathbb{E}[\deg(0, u)^2] du < \infty$.

Next, we deal with the second term and note that the covariance in the integrand is given by

$$\begin{aligned} \text{Cov}(\text{deg}(x, u), \text{deg}(y, v)) &= \mathbb{E} \left[\sum_{P' \in \mathcal{P}'} \mathbb{1}\{P' \in B(\{(x, u), (y, v)\})\} \right] \\ &+ \mathbb{E} \left[\sum_{P'_1 \neq P'_2 \in \mathcal{P}'} \mathbb{1}\{P'_1 \in B(x, u), P'_2 \in B(y, v)\} \right] - \mathbb{E} \left[\sum_{P' \in \mathcal{P}'} \mathbb{1}\{P' \in B(x, u)\} \right] \mathbb{E} \left[\sum_{P' \in \mathcal{P}'} \mathbb{1}\{P' \in B(y, v)\} \right] \\ &= \lambda' \int_{\mathbb{S}} \mathbb{1}\{p' \in B(\{(x, u), (y, v)\})\} dp' = \lambda' |B(\{(x, u), (y, v)\})|. \end{aligned}$$

From Lemma 6.1 with $m = 1$ and translation invariance, we obtain that

$$\int_{A \times [0, 1]} \int_{\mathbb{S}} |B(\{(x, u), (y, v)\})| d(x, u) d(y, v) = \frac{1}{1 - 2\gamma'} \frac{(2\beta)^2}{1 - \gamma} \int_0^1 u^{-\gamma} du < \infty.$$

Hence, $\text{Var}(T_1) = \text{Var}(S([0, 1])) < \infty$. Similarly, we obtain that

$$\begin{aligned} \sum_{k \geq 2} \text{Cov}(T_1, T_k) &= \mathbb{E} \left[\sum_{\substack{P_i \in \mathcal{P} \cap [0, 1] \times [0, 1], \\ P_j \in \mathcal{P} \cap [1, \infty) \times [0, 1]}} \text{deg}(P_i) \text{deg}(P_j) \right] - \mathbb{E} \left[\sum_{P_i \in \mathcal{P} \cap A} \text{deg}(P_i) \right]^2 \\ &\leq \int_{[0, 1]^2} \int_{\mathbb{S}} \text{Cov}(\text{deg}(x, u), \text{deg}(y, v)) d(y, v) d(x, u) \leq \frac{1}{1 - 2\gamma'} \left(\frac{2\beta}{1 - \gamma} \right)^2 \int_0^1 u^{-\gamma} du < \infty, \end{aligned}$$

thereby showing the finiteness of $\sum_{k \geq 1} \text{Cov}(T_1, T_k)$. \square

6.2. Proof of Theorem 2.5— stable limit. The idea of the proof of Theorem 2.5(b) is to apply [27, Theorem 4.5.2], which says the following. Let $X_i, i \geq 1$ be iid nonnegative random variables with $\mathbb{P}(X_1 > x) \sim Ax^{-\alpha}$ for some $\alpha \in (1, 2)$ and $A > 0$. Then $n^{-1/\alpha} \sum_{i \leq n} (X_i - \mathbb{E}[X_i])$ converges in distribution to an α -stable random variable.

Proof of Theorem 2.5(b). Let $u_n := n^{-b}$ for an arbitrary choice of $b \in (2/3, 1)$. Decompose S_n into

$$S_n = S_n^{\geq} + S_n^{\leq} := \sum_{P \in \mathcal{P} \cap \mathbb{S}_{n, \geq u_n}} \text{deg}(P) + \sum_{P \in \mathcal{P} \cap \mathbb{S}_{n, \leq u_n}} \text{deg}(P),$$

where $\mathbb{S}_{n, \geq u} := [0, n] \times [u, 1]$ and $\mathbb{S}_{n, \leq u} := [0, n] \times [0, u]$.

First, we show that $n^{-\gamma}(S_n^{\geq} - \mathbb{E}[S_n^{\geq}])$ converges to 0 in probability as $n \rightarrow \infty$. By Chebychev's inequality, this follows once we have shown that $\text{Var}(S_n^{\geq}) \in o(n^{2\gamma})$. Note that

$$\text{Var}(S_n^{\geq}) = \lambda \int_{\mathbb{S}_{n, \geq u_n}} \mathbb{E}[\text{deg}(x, u)^2] d(x, u) + \lambda^2 \iint_{\mathbb{S}_{n, \geq u_n}^2} \text{Cov}(\text{deg}(x, u), \text{deg}(y, u)) d(x, u) d(y, v) \quad (6.1)$$

Here, by translation invariance, the first term is bounded by $(nu_n^{1-2\gamma})/(1 - 2\gamma)$, which is in $o(n^{2\gamma})$ since $1 - b(1 - 2\gamma) < 2\gamma$, which holds for all $b < 1$ and $\gamma > 1/2$. For the second term, Lemma 6.1 gives the bound

$$2n\lambda^2 \int_{u_n}^1 \int_{\mathbb{S}_{\geq u}} |B(\{(0, u), (y, v)\})| d(y, v) du \in O(n),$$

where $\mathbb{S}_{\geq u} := \mathbb{R} \times [u, 1]$. Thus, $n^{-\gamma}(S_n^{\geq} - \mathbb{E}[S_n^{\geq}]) \xrightarrow{\mathbb{P}} 0$.

For $u \leq 1$, we set $\mu(u) := \mathbb{E}[\text{deg}(0, u)] = (2\beta u^{-\gamma})/(1 - \gamma')$ and

$$S_n^{(1)} := \sum_{(X, U) \in \mathcal{P} \cap \mathbb{S}_{n, \leq u_n}} \mu(U) \quad \text{and} \quad S_n^{(2)} := \sum_{i \leq \lfloor \lambda n \rfloor} \mu(U_i) \mathbb{1}\{U_i \leq u_n\},$$

where U_1, U_2, \dots are iid uniforms on $[0, 1]$. We next prove that $\mathbb{E}[|S_n^{\leq} - S_n^{(1)}|] + \mathbb{E}[|S_n^{(1)} - S_n^{(2)}|] \in o(n^\gamma)$. For the first expectation, note that, by the Mecke equation,

$$\mathbb{E}[|S_n^{\leq} - S_n^{(1)}|] \leq n\lambda \int_0^{u_n} \mathbb{E}[|\text{deg}(0, u) - \mu(u)|] du \leq n\lambda \int_0^{u_n} \sqrt{\text{Var}(\text{deg}(0, u))} du = n\lambda \int_0^{u_n} \sqrt{\mu(u)} du, ,$$

Therefore, $\mathbb{E}[|S_n^{\leq} - S_n^{(1)}|] \in O(nu_n^{1-\gamma/2})$. Since $1 - b(1 - \gamma/2) < \gamma$, which holds for $b > 2/3$, we conclude that $n^{-\gamma} \mathbb{E}[|S_n^{\leq} - S_n^{(1)}|] \rightarrow 0$.

Second, we obtain with a Poisson random variable N with parameter λn ,

$$\mathbb{E}[|S_n^{(1)} - S_n^{(2)}|] \leq \mathbb{E}[|N - \lceil \lambda n \rceil|] \int_0^{u_n} \mu(u) du \leq (\sqrt{\text{Var}(N)} + 1) \int_0^{u_n} \mu(u) du.$$

Now, $\text{Var}(N) = \lambda n$ and the integral above is in $O(u_n^{1-\gamma})$. Therefore, $\mathbb{E}[|S_n^{(1)} - S_n^{(2)}|] \in O(\sqrt{\lambda n} u_n^{1-\gamma})$. Since $1/2 - b(1-\gamma) < \gamma$, which holds for all b if $\gamma > 1/2$, it follows that $n^{-\gamma} \mathbb{E}[|S_n^{(1)} - S_n^{(2)}|] \rightarrow 0$.

It therefore suffices to prove that $n^{-\gamma}(S_n^{(2)} - \mathbb{E}[S_n^{(2)}])$ converges in distribution to a stable random variable. Note that by [14, Lemma 11],

$$\sum_{i \leq \lceil \lambda n \rceil} \mu(U_i) \mathbb{1}\{U_i > u_n\} \xrightarrow{L^2} 0 \quad \text{as } n \rightarrow \infty.$$

Finally, [27, Theorem 4.5.2] implies that $n^{-\gamma-1} \sum_{i \leq \lceil \lambda n \rceil} (\mu(U_i) - \mathbb{E}[\mu(U_i)])$ converges in distribution to a γ^{-1} -stable random variable. \square

7. PROOF OF THEOREM 2.6

We now extend the proof of Theorem 2.5 to the case of m -simplices. More precisely, we consider

$$S_n := \sum_{P \in \mathcal{P} \cap \mathbb{S}_n} d_m(P),$$

where for $p = (x, u)$, we set

$$d_m(p) := \frac{1}{m!} \sum_{(P_1, \dots, P_m) \in (\mathcal{P} \cap \mathbb{S}_{>u})^m} \mathbb{1}\{\mathcal{P}' \cap B(\{p, P_1, \dots, P_m\}) \neq \emptyset\}$$

is the number of m -simplices containing p .

Lemma 7.1 (Moment computations). *Let $m \geq 1$. Then,*

- (a) $\mathbb{E}[d_m(0, u)^2] \in O(u^{-2\gamma})$.
- (b) $\mathbb{E}[\text{Var}(d_m(0, u) | \mathcal{P}')] \in O(u^{1-3\gamma})$.
- (c) $\int_{\mathbb{S}} |\mathbb{E}[\text{Cov}(d_m(0, u), d_m(p) | \mathcal{P}')]| dp \in O(u^{1-3\gamma})$.
- (d) $\text{Var}(\mathbb{E}[d_m(0, u) | \mathcal{P}']) \in O(u^{-\gamma})$.
- (e) $\int_{\mathbb{S}} |\text{Cov}(\mathbb{E}[d_m(0, u) | \mathcal{P}'], \mathbb{E}[d_m(p) | \mathcal{P}'])| dp \in O(u^{-\gamma})$.

We defer the technical computations to the end of this section and first explain how to conclude the proof of Theorem 2.6 based on Lemma 7.1. For $\gamma < 1/2$, we follow the same strategy as in the proof of Theorem 2.5(a).

Proof of Theorem 2.6(a). Let

$$T_i := \sum_{P_j \in [i-1, i] \times [0, 1]} d_m(P_j).$$

We apply [27, Theorem 4.4.3] which holds for sequences of identically distributed associated random variables T_1, T_2, \dots , and need to show that $\sum_{k \geq 1} \text{Cov}(T_1, T_k) < \infty$.

By the formula for the total variance, we have $\text{Var}(T_1) = \mathbb{E}[\text{Var}(T_1 | \mathcal{P}')] + \text{Var}(\mathbb{E}[T_1 | \mathcal{P}'])$, where by Lemma 7.1 (a), (c), and translation invariance

$$\mathbb{E}[\text{Var}(T_1 | \mathcal{P}')] = \lambda \int_{\mathbb{S}_1} \mathbb{E}[d_m(p)^2] dp + \lambda^2 \iint_{\mathbb{S}_1^2} \mathbb{E}[\text{Cov}(d_m(p_1), d_m(p_2) | \mathcal{P}')] dp_1 dp_2 < \infty.$$

Moreover, by part (e) of Lemma 7.1 and translation invariance,

$$\text{Var}(\mathbb{E}[T_1 | \mathcal{P}']) = \lambda^2 \iint_{\mathbb{S}_1^2} \text{Cov}(\mathbb{E}[d_m(p_1) | \mathcal{P}'], \mathbb{E}[d_m(p_2) | \mathcal{P}']) dp_1 dp_2 < \infty.$$

Analogously, we obtain that

$$\begin{aligned} \sum_{k \geq 2} \text{Cov}(T_1, T_k) &= \sum_{k \geq 2} \{ \mathbb{E}[\text{Cov}(T_1, T_k \mid \mathcal{P}')] + \text{Cov}(\mathbb{E}[T_1 \mid \mathcal{P}'], \mathbb{E}[T_k \mid \mathcal{P}']) \} \\ &= \lambda^2 \int_{\mathbb{S}_1} \int_{[1, \infty) \times [0, 1]} \mathbb{E}[\text{Cov}(d_m(p_1), d_m(p_2) \mid \mathcal{P}')] dp_1 dp_2 \\ &\quad + \lambda^2 \int_{\mathbb{S}_1} \int_{[1, \infty) \times [0, 1]} \text{Cov}(\mathbb{E}[d_m(p_1) \mid \mathcal{P}'], \mathbb{E}[d_m(p_2) \mid \mathcal{P}']) dp_1 dp_2 < \infty. \end{aligned}$$

□

Next, we prove Theorem 2.6(b).

Proof of Theorem 2.6(b). The idea is to proceed analogously to the proof of Theorem 2.3(b). We assume that $\gamma' < 1/(2m+1)$, and choose $u_n = n^{-b}$, where $b \in (2/3, 1)$, similarly as in the proof of Theorem 2.5. Then, we split S_n into

$$S_n = S_n^{\geq} + S_n^{\leq} := \sum_{P_i \in \mathcal{P} \cap \mathbb{S}_{n, \geq u_n}} d_m(P_i) + \sum_{P_i \in \mathcal{P} \cap \mathbb{S}_{n, \leq u_n}} d_m(P_i).$$

We now show that $n^{-\gamma}(S_n^{\geq} - \mathbb{E}[S_n^{\geq}])$ converges to 0 in probability. This follows, as soon as we have proved that $\text{Var}(S_n^{\geq}) \in o(n^{2\gamma})$. We have

$$\text{Var}(S_n^{\geq}) = n\lambda \int_{u_n}^1 \mathbb{E}[d_m(0, u)^2] du + n\lambda^2 \int_{\mathbb{S}_{1, \geq u_n}} \int_{\mathbb{S}_{n, \geq u_n}} |\text{Cov}(d_m(x, u), d_m(p))| dp d(x, u).$$

By Lemma 7.1 (a), (c), and translation invariance, there are constants $c_1, c_2 > 0$ such that the above is bounded by

$$c_1 n\lambda \int_{u_n}^1 u^{-2\gamma} du + c_2 n\lambda^2 \int_{u_n}^1 u^{1-3\gamma} du \in O(nu_n^{1-2\gamma}),$$

which is in $o(n^{2\gamma})$, since $1 - b(1 - 2\gamma) < 2\gamma$ for $\gamma > 1/2$. Thus, $n^{-\gamma}(S_n^{\geq} - \mathbb{E}[S_n^{\geq}]) \xrightarrow{\mathbb{P}} 0$. Next, we let

$$S_n^{(1)} := \sum_{(X, U) \in \mathcal{P} \cap \mathbb{S}_n} \mu_m(U), \quad S_n^{(2)} := \sum_{i \leq n} \mu_m(U_i) \mathbb{1}\{U_i \leq u_n\},$$

where $\mu_m(u) := \mathbb{E}[d_m(0, u)]$, and U_1, U_2, \dots are iid uniform random variables on $[0, 1]$. We next prove that $\mathbb{E}[|S_n^{\leq} - S_n^{(1)}|] + \mathbb{E}[|S_n^{(1)} - S_n^{(2)}|] \in o(n^\gamma)$. For the first expectation, note that by the Mecke equation,

$$\mathbb{E}[|S_n^{\leq} - S_n^{(1)}|] \leq n\lambda \int_0^{u_n} \mathbb{E}[|d_m(0, u) - \mu_m(u)|] du \leq n\lambda \int_0^{u_n} \sqrt{\text{Var}(\text{deg}_m(0, u))} du.$$

From Lemma 7.1 (b), (d), we have that $\text{Var}(\text{deg}_m(0, u)) \in O(u^{1-3\gamma})$. Hence,

$$\mathbb{E}[|S_n^{\leq} - S_n^{(1)}|] \leq nu_n^{3(1-\gamma)/2} \in o(n^\gamma),$$

since $1 - b(3(1-\gamma)/2) < \gamma$ for $b > 2/3$. From here, we conclude the proof as in Theorem 2.5. □

Finally, we conclude by proving Lemma 7.1. We note that the proof of (b) is largely parallel to (c), and the proof of (d) is largely parallel to (e). Nevertheless, to make the manuscript self-contained, we provide the details.

Proof of Lemma 7.1. Henceforth, we use the abbreviations $\mathbf{p}_{i,m} := (p_{m-i+1}, \dots, p_{2m-i})$, $\overrightarrow{\mathbf{p}}_{i,m} := \{p_{m-i+1}, \dots, p_{2m-i}\}$, and $\overrightarrow{\mathbf{p}}_{i,m}(u) := \{(0, u), p_{m-i+1}, \dots, p_{2m-i}\}$. Furthermore, to ease notation, we introduce for a set A the abbreviation $\mathcal{P}'_A := \mathcal{P}' \cap B(A)$.

(a) Conditioned on \mathcal{P}' , $d_m(0, u)$ is a U -statistic. Therefore, by [21, Lemma 3.5] with $k_i := 1/(i!(m-i)!)^2$,

$$\mathbb{E}[d_m(0, u)^2 \mid \mathcal{P}'] = \sum_{i=0}^m \lambda^{2m-i} k_i \int_{\mathbb{S}_{\geq u}^{2m-i}} \mathbb{P}(\mathcal{P}'_{\overrightarrow{\mathbf{p}}_m(u)} \neq \emptyset, \mathcal{P}'_{\overrightarrow{\mathbf{p}}_{i,m}(u)} \neq \emptyset \mid \mathcal{P}') d\mathbf{p}_{2m-i}.$$

Therefore,

$$\begin{aligned}\mathbb{E}[d_m(0, u)^2] &= \sum_{i=0}^m \lambda^{2m-i} k_i \int_{\mathbb{S}_{\geq u}^{2m-i}} \mathbb{P}(\mathcal{P}'_{\mathbf{p}_m(u)} \neq \emptyset, \mathcal{P}'_{\mathbf{p}_{i,m}(u)} \neq \emptyset) d\mathbf{p}_{2m-i} \\ &\leq \sum_{i=0}^m \lambda^{2m-i} k_i \int_{\mathbb{S}_{\geq u}^{2m-i}} (\mathbb{P}(\mathcal{P}'_{\mathbf{p}_{2m-i}(u)} \neq \emptyset) + \mathbb{P}(\mathcal{P}'_{\mathbf{p}_m(u)} \neq \emptyset) \mathbb{P}(\mathcal{P}'_{\mathbf{p}_{i,m}(u)} \neq \emptyset)) d\mathbf{p}_{2m-i},\end{aligned}$$

where we used that for all Borel sets $A, B \subseteq \mathbb{S}$, $\mathbb{P}(\mathcal{P}' \cap A \neq \emptyset, \mathcal{P}' \cap B \neq \emptyset) = \mathbb{P}(\mathcal{P}' \cap A \cap B \neq \emptyset) + \mathbb{P}(\mathcal{P}' \cap A \setminus B \neq \emptyset, \mathcal{P}' \cap B \setminus A \neq \emptyset)$. Next, we use that for all Borel set $A \subseteq \mathbb{R} \times [0, 1]$, $\mathbb{P}(\mathcal{P}' \cap A = \emptyset) \leq \lambda'|A|$ and obtain that the above is bounded by

$$\sum_{k=m}^{2m} \lambda^k \int_{\mathbb{S}_{\geq u}^k} (\lambda'|B(\overrightarrow{\mathbf{p}}_k(u))| + (\lambda')^2|B(\overrightarrow{\mathbf{p}}_m(u))||B(\{(0, u), p_{m+1}, \dots, p_k\})|) d\mathbf{p}_k,$$

which is of order $O(u^{-2\gamma})$ by Lemma 6.1.

(b) By [21, Lemma 3.5],

$$\text{Var}(d_m(0, u) \mid \mathcal{P}') = \sum_{i=1}^m \lambda^{2m-i} k_i \int_{\mathbb{S}_{\geq u}^{2m-i}} \mathbb{1}\{\mathcal{P}'_{\mathbf{p}_m(u)} \neq \emptyset\} \mathbb{1}\{\mathcal{P}'_{\mathbf{p}_{i,m}(u)} \neq \emptyset\} d\mathbf{p}_{2m-i}.$$

Therefore,

$$\mathbb{E}[\text{Var}(d_m(0, u) \mid \mathcal{P}')] = \sum_{i=1}^m \lambda^{2m-i} k_i \int_{\mathbb{S}_{\geq u}^{2m-i}} \mathbb{P}(\mathcal{P}'_{\mathbf{p}_m(u)} \neq \emptyset, \mathcal{P}'_{\mathbf{p}_{i,m}(u)} \neq \emptyset) d\mathbf{p}_{2m-i}.$$

Similarly, as in part (a), we find that the above is bounded by

$$\begin{aligned}\sum_{i=1}^m \lambda^{2m-i} k_i \int_{\mathbb{S}_{\geq u}^{2m-i}} (\mathbb{P}(\mathcal{P}'_{\mathbf{p}_{2m-i}(u)} \neq \emptyset) + \mathbb{P}(\mathcal{P}'_{\mathbf{p}_m(u)} \neq \emptyset) \mathbb{P}(\mathcal{P}'_{\{(0, u), p_{m-i+1}, \dots, p_{2m-i}\}} \neq \emptyset)) d\mathbf{p}_{2m-i} \\ \leq \sum_{i=1}^m \lambda^{2m-i} k_i \int_{\mathbb{S}_{\geq u}^{2m-i}} (\lambda'|B(\overrightarrow{\mathbf{p}}_{2m-i}(u))| + (\lambda')^2|B(\overrightarrow{\mathbf{p}}_m(u))||B(\{p_m, \dots, p_{2m-i}\})|) d\mathbf{p}_{2m-i},\end{aligned}$$

where the last inequality follows by the same argument as in part (a). Recall that $\overrightarrow{\mathbf{p}}_{i,m}(u) = \{(0, u), p_{m-i+1}, \dots, p_{2m-i}\}$. Next, we apply Lemma 6.1 to $|B(\overrightarrow{\mathbf{p}}_{2m-1}(u))|$, integrated with respect to \mathbf{p}_{2m-1} , and to $|B(\overrightarrow{\mathbf{p}}_{1,m})|$, integrated with respect to p_{m+1}, \dots, p_{2m-i} . This gives

$$\lambda^m (\lambda')^2 \left(\sum_{i=1}^m k_i \frac{(2\beta)^{m-i+1}}{(1-\gamma)^{m-i}} \frac{1}{1-(m-i+1)\gamma'} \right) \int_{\mathbb{S}_{\geq u}^m} v_m^{-\gamma} |B(\overrightarrow{\mathbf{p}}_m(u))| d\mathbf{p}_m + O(u^{-\gamma}),$$

where $p_m := (y_m, v_m)$. Moreover, for all $u \in [0, 1]$,

$$\begin{aligned}\int_{\mathbb{S}_{\geq u}^m} v_m^{-\gamma} |B(\overrightarrow{\mathbf{p}}_m(u))| d\mathbf{p}_m \\ = \int_{\mathbb{S}} \int_{\mathbb{S}_{\geq u}^m} v_m^{-\gamma} \mathbb{1}\{|z| \leq \beta w^{-\gamma'} u^{-\gamma}\} \prod_{i=1}^m \mathbb{1}\{|z - y_i| \leq \beta w^{-\gamma'} v_i^{-\gamma}\} d((y_1, v_1), \dots, (y_m, v_m)) d(z, w) \\ \leq (2\beta)^m \int_{\mathbb{S}} \int_{[0,1]^{m-1} \times [u,1]} w^{-m\gamma'} v_1^{-\gamma} \dots v_{m-1}^{-\gamma} v_m^{-2\gamma} \mathbb{1}\{|z| \leq \beta w^{-\gamma'} u^{-\gamma}\} d(v_1, \dots, v_m) d(z, w) \\ = \frac{(2\beta)^{m+1} (u^{1-2\gamma} - 1) u^{-\gamma}}{(1-\gamma)^{m-1} (2\gamma - 1)} \int_0^1 w^{-(m+1)\gamma'} dw = \frac{(2\beta)^{m+1} (u^{1-2\gamma} - 1) u^{-\gamma}}{(1-\gamma)^{m-1} (2\gamma - 1) (1 - (m+1)\gamma')},\end{aligned}\tag{7.1}$$

which shows that $\mathbb{E}[\text{Var}(d_m(0, u) \mid \mathcal{P}')] \in O(u^{1-3\gamma})$.

- (c) From the polarization identity $\text{Cov}(X, Y) = 1/4(\text{Var}(X + Y) - \text{Var}(X - Y))$ and [21, Lemma 3.5] (applied to the U -statistics $d_m(0, u) + d_m(p)$ and $d_m(0, u) - d_m(p)$) we obtain that

$$\begin{aligned} & \int_{\mathbb{S}} \text{Cov}(d_m(0, u), d_m(p) | \mathcal{P}') \, dp \\ &= \sum_{i=1}^m \lambda^{2m-i} k_i \int_{\mathbb{S}} \int_{\mathbb{S}_{\geq u}^m \times \mathbb{S}_{\geq v}^{m-i}} \mathbb{1}\{\mathcal{P}'_{\overrightarrow{\mathbf{p}}_m(u)} \neq \emptyset\} \mathbb{1}\{\mathcal{P}'_{\{p, p_{m-i+1}, \dots, p_{2m-i}\}} \neq \emptyset\} \, d\mathbf{p}_{2m-i} \, dp, \end{aligned}$$

where $p := (y, v)$. Therefore, analogously to part (b),

$$\begin{aligned} & \int_{\mathbb{S}} |\mathbb{E}[\text{Cov}(d_m(0, u), d_m(p) | \mathcal{P}')]| \, dp \\ & \leq \sum_{i=1}^m \lambda^{2m-i} k_i \int_{\mathbb{S}} \int_{\mathbb{S}_{\geq u}^m \times \mathbb{S}_{\geq v}^{m-i}} (\lambda' |B(\overrightarrow{\mathbf{p}}_{2m-i}(u))| + (\lambda')^2 |B(\overrightarrow{\mathbf{p}}_m(u))| |B(\{p, p_m, \dots, p_{2m-i}\})|) \, d\mathbf{p}_{2m-i} \, dp. \end{aligned}$$

Now, we apply Lemma 6.1 to $|B(\overrightarrow{\mathbf{p}}_{2m-i}(u))|$ (integrated with respect to \mathbf{p}_{2m-i}) and to $|B(\{p, p_m, \dots, p_{2m-i}\})|$ (integrated with respect to $(p, p_{m+1}, \dots, p_{2m-i})$). This gives

$$\lambda^m (\lambda')^2 \left(\sum_{i=1}^m k_i \frac{(2\beta)^{m-i+2}}{(1-\gamma)^{m-i+1}} \frac{1}{1 - (m-i+2)\gamma'} \right) \int_{\mathbb{S}_{\geq u}^m} v_m^{-\gamma} |B(\overrightarrow{\mathbf{p}}_m(u))| \, d\mathbf{p}_m + O(u^{-\gamma}).$$

From here, $\int_{\mathbb{S}} \mathbb{E}[\text{Cov}(d_m(0, u), d_m(p) | \mathcal{P}')] \, dp \in O(u^{1-3\gamma})$ follows analogously to (7.1) as asserted.

- (d) We have that

$$\mathbb{E}[d_m(0, u) | \mathcal{P}'] = \frac{\lambda^m}{m!} \int_{\mathbb{S}_{\geq u}^m} \mathbb{1}\{\mathcal{P}'_{\overrightarrow{\mathbf{p}}_m(u)} \neq \emptyset\} \, d\mathbf{p}_m,$$

and therefore,

$$\text{Var}(\mathbb{E}[d_m(0, u) | \mathcal{P}']) = \frac{\lambda^{2m}}{(m!)^2} \int_{\mathbb{S}_{\geq u}^{2m}} \text{Cov}(\mathbb{1}\{\mathcal{P}'_{\overrightarrow{\mathbf{p}}_m(u)} \neq \emptyset\}, \mathbb{1}\{\mathcal{P}'_{\overrightarrow{\mathbf{p}}_{0,m}(u)} \neq \emptyset\}) \, d\mathbf{p}_{2m}. \quad (7.2)$$

Now, we use that $\text{Cov}(XY, XZ) = \mathbb{E}[Y]\mathbb{E}[Z]\text{Var}(X)$ for independent X, Y, Z . We let

$$\begin{aligned} X &:= \mathbb{1}\{\mathcal{P}'_{\overrightarrow{\mathbf{p}}_{2m}(u)} \neq \emptyset\}, \\ Y &:= \mathbb{1}\{\mathcal{P}' \cap (B(\overrightarrow{\mathbf{p}}_m(u)) \setminus B(\overrightarrow{\mathbf{p}}_{0,m}(u))) \neq \emptyset\}, \\ Z &:= \mathbb{1}\{\mathcal{P}' \cap (B(\overrightarrow{\mathbf{p}}_{0,m}(u)) \setminus B(\overrightarrow{\mathbf{p}}_m(u))) \neq \emptyset\}, \end{aligned}$$

and deduce that

$$\begin{aligned} \text{Var}(\mathbb{E}[d_m(0, u) | \mathcal{P}']) &= \frac{\lambda^{2m}}{m!} \int_{\mathbb{S}_{\geq u}^{2m}} \mathbb{P}(\mathcal{P}' \cap (B(\overrightarrow{\mathbf{p}}_m(u)) \cup B(\overrightarrow{\mathbf{p}}_{0,m}(u))) \neq \emptyset) \mathbb{P}(\mathcal{P}'_{\overrightarrow{\mathbf{p}}_{2m}(u)} \neq \emptyset) \, d\mathbf{p}_{2m} \\ &\leq \frac{\lambda^{2m} \lambda'}{m!} \int_{\mathbb{S}_{\geq u}^{2m}} |B(\overrightarrow{\mathbf{p}}_{2m}(u))| \, d\mathbf{p}_{2m}, \end{aligned} \quad (7.3)$$

which shows by Lemma 6.1 that $\text{Var}(\mathbb{E}[d_m(0, u) | \mathcal{P}']) \in O(u^{-\gamma})$.

- (e) Analogously to (7.2), we find that

$$\begin{aligned} & \int_{\mathbb{S}} |\text{Cov}(\mathbb{E}[d_m(0, u) | \mathcal{P}'], \mathbb{E}[d_m(p) | \mathcal{P}'])| \, dp \\ &= \lambda^{2m} \int_{\mathbb{S}} \int_{\mathbb{S}_{\geq u}^m \times \mathbb{S}_{\geq v}^m} |\text{Cov}(\mathbb{1}\{\mathcal{P}'_{\overrightarrow{\mathbf{p}}_m(u)} \neq \emptyset\}, \mathbb{1}\{\mathcal{P}'_{\{p\} \cup \overrightarrow{\mathbf{p}}_{i,m}} \neq \emptyset\})| \, d\mathbf{p}_{2m} \, dp, \end{aligned}$$

where $p = (y, v)$. Here, we apply the relation $\text{Cov}(XY, XZ) = \mathbb{E}[Y]\mathbb{E}[Z]\text{Var}(X)$ with

$$\begin{aligned} X &:= \mathbb{1}\{\mathcal{P}'_{\{p\} \cup \overrightarrow{\mathbf{p}}_{2m}(u)} \neq \emptyset\}, \\ Y &:= \mathbb{1}\{\mathcal{P}' \cap (B(\overrightarrow{\mathbf{p}}_m(u)) \setminus B(\{p\} \cup \overrightarrow{\mathbf{p}}_{0,m})) \neq \emptyset\}, \\ Z &:= \mathbb{1}\{\mathcal{P}' \cap (B(\{p\} \cup \overrightarrow{\mathbf{p}}_{0,m}) \setminus B(\overrightarrow{\mathbf{p}}_m(u))) \neq \emptyset\}, \end{aligned}$$

and deduce analogously to (7.3) that

$$\int_{\mathbb{S}} |\text{Cov}(\mathbb{E}[d_m(0, u) | \mathcal{P}'], \mathbb{E}[d_m(p) | \mathcal{P}'])| dp \leq \lambda^{2m} \int_{\mathbb{S}} \int_{\mathbb{S}_{\geq u}^m \times \mathbb{S}_{\geq v}^m} |B(\{p\} \cup \overrightarrow{p_{2m}}(u))| d\mathbf{p}_{2m} dp,$$

which is by Lemma 6.1 of order $O(u^{-\gamma})$. □

8. SIMULATION STUDY

To see how the theoretical results can be applied to networks of finite size, in this section we present a simulation study where we analyze finite networks and Palm distributions.

To analyze the statistical properties of the model, we utilize a Monte Carlo approach: we implemented a C++ algorithm to generate several higher-order networks with identical model parameters. The simulation of a finite network consists of the following steps:

- (1) We first construct a torus of dimension 1, and generate two Poisson point processes \mathcal{P} , \mathcal{P}' . For practical reasons, we do not keep the intensity measures λ and λ' of the Poisson point processes constant throughout the simulations, but rather generate the network samples on a torus of Lebesgue measure 1, and adjust the Poisson intensity measures accordingly to generate networks with different expected number of \mathcal{P} - and \mathcal{P}' -vertices. After generating \mathcal{P} and \mathcal{P}' , the vertices are equipped with a mark uniformly distributed in $[0, 1]$.
- (2) Then, we generate the connections between the \mathcal{P} - and \mathcal{P}' -vertices using the connection rule described in (2.2). By using periodic boundary conditions, we can treat the vertices equivalently, irrespective to their position in the torus. Note that the parameter β can be tuned to adjust the expected number of edges in the network. The expected Δ_0 -degree of a point $o = (0, u)$ is given by

$$\mathbb{E}\left[\sum_{p' \in \mathcal{P}'} \mathbf{1}\{p' \in B(o)\}\right] = 2\beta\lambda' / ((1 - \gamma)(1 - \gamma')),$$

where we followed the same arguments as in the proof of 6.1, with $m = 0$.

- (3) Finally, we construct the higher-order network on \mathcal{P} , where the set of m -simplices is determined according to (2.4).

The simulation of the network is computationally expensive. If we checked the connection condition for every \mathcal{P} - and \mathcal{P}' -vertex pair, our algorithm would have a time complexity of $O(\lambda\lambda')$, where λ and λ' are the intensity of the Poisson processes for the \mathcal{P} - and \mathcal{P}' -vertices, respectively. When deciding which points in \mathcal{P} and \mathcal{P}' are connected, we partition the space \mathbb{S} to rectangles containing multiple points, similarly for the quadtree data structures [22]. This way, we can reduce the computational complexity of the simulation as

- if the furthest points of two rectangles with the highest marks connect, it is certain that all point pairs in the rectangles are connected;
- if the closest points of two rectangles with the lowest marks do not connect, it is certain that no point pairs in the rectangles are connected.

The width of the rectangles is set to be proportional to $b^{-\gamma}$ and $b^{-\gamma'}$ for the \mathcal{P} - and \mathcal{P}' -vertices, respectively, where b denotes the bottom mark of the rectangle. This results in a layout of rectangles as shown in Figure 1.

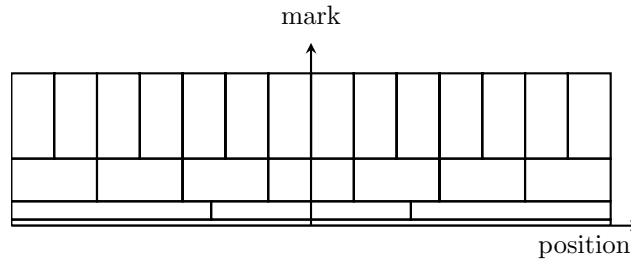


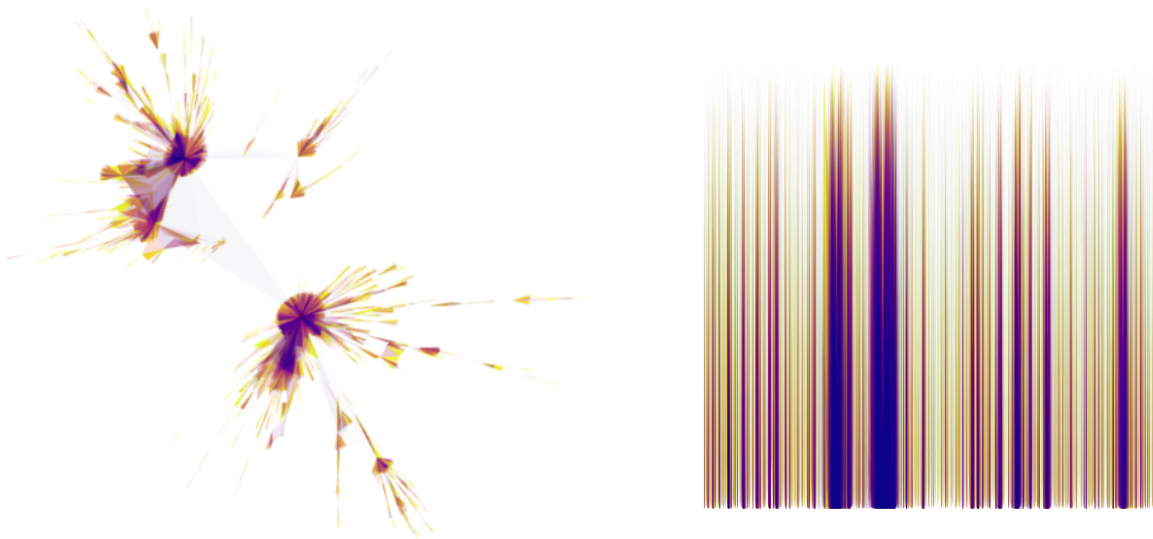
FIGURE 1. Partition of \mathbb{S} to rectangles.

Before generating a finite network sample, we set the model parameters so that they are of the same order of magnitude when fitted to the analyzed datasets. The intensity measures of the Poisson point processes are set to $\lambda = \lambda' = 100\,000$. Aligned with these parameters, the number of \mathcal{P} - and \mathcal{P}' -vertices were 100 335 and 93 919, respectively. The γ, γ' model parameters were set to $\gamma = 0.7, \gamma' = 0.2$. Furthermore, β was set so that the expected number of Δ_0 -degrees in the infinite network limit was 3: $\beta = 3.6E - 5$.

First, we examine three degree distributions of the networks, which are analyzed in Theorem 2.3.

- The Δ_0 -degree distribution characterizes the distribution of the number of \mathcal{P}' -vertices connected to a typical \mathcal{P} -vertex.
- The Δ_1 -degree distribution is the distribution of the number of \mathcal{P}' -vertices connected to a pair of \mathcal{P} -vertices.
- Finally, the distribution of the number of \mathcal{P} -vertices connected to a typical \mathcal{P}' -vertex is described by the Δ'_0 -degree distribution.

The main characteristics of a network generated with these parameters is shown in Figure 2. In the top row of Figure 2, one can see the largest component of the network (left). A polygon is drawn representing the convex hull of a set of \mathcal{P} -vertices whenever they form a simplex in the network. The higher number of \mathcal{P} -vertices forms a simplex, the darker color the corresponding polygon has. From the largest component of the network, which contained 12 385 \mathcal{P} -vertices, one can see that the network is sparse, and that the network layout is dominated by a few dense regions corresponding to \mathcal{P} -vertices with high degrees.



The largest component of a network sample

Network sample with fixed positions

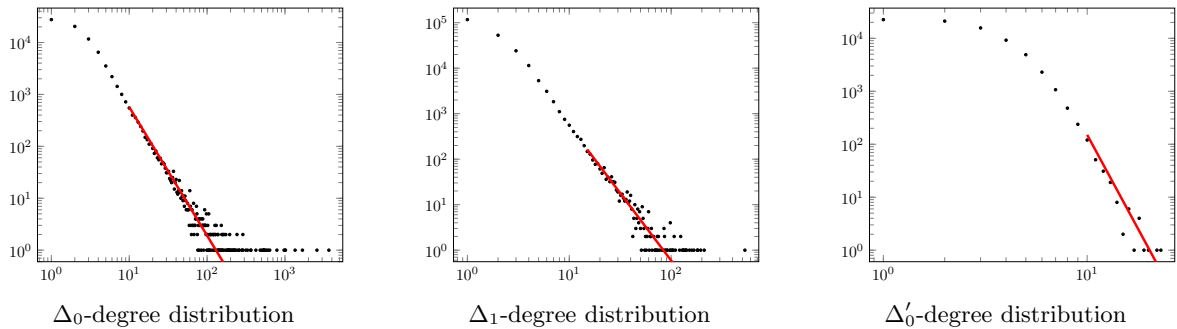


FIGURE 2. Main properties of a network sample generated by our model

When looking at the positions of the \mathcal{P} -vertices embedded in the space \mathbb{S} (right), one can see that the \mathcal{P} -vertices form clusters that are connected by the above-mentioned heavy vertices. As illustrated in the bottom row of 2, the various degree distributions of the \mathcal{P} - and \mathcal{P}' -vertices are all heavy tailed, and that the degree distribution of the \mathcal{P} -vertices is heavier than the degree distribution of the \mathcal{P}' -vertices, aligned with our theoretical results.

We also rely on Palm calculus to simulate typical simplices in networks devoid of finite-size effects. To do so, we first place a typical \mathcal{P} -vertex $(0, u)$ to the origin. Then, we simulate \mathcal{P}' -vertices $(y_1, v_1), \dots, (y_n, v_n) \in B(0, u)$ in its neighborhood where \mathcal{P}' -vertices connect to it, where n is a Poisson distributed random variable with parameter $\lambda'|B(0, u)|$. Finally, further \mathcal{P} -vertices are generated by a Poisson process of intensity λ in the union of the neighborhoods $\bigcup_i N(y_i, v_i)$ of the \mathcal{P}' -vertices. Each of the neighborhoods $N(y_i, v_i)$ can be split to three parts, where a connecting \mathcal{P} -vertex (x, w) must satisfy the below conditions:

$$\begin{array}{ll} \text{left tail} & w \leq (y_i - x)/\beta v_i^{-\gamma'} \quad x < y_i - \beta v_i^{-\gamma'}; \\ \text{center} & w \leq 1 \quad y_i - \beta v_i^{-\gamma'} \leq x \leq y_i + \beta v_i^{-\gamma'}; \\ \text{right tail} & w \leq (x - y_i)/\beta v_i^{-\gamma'} \quad y_i + \beta v_i^{-\gamma'} < x. \end{array}$$

Next, we take the union of the center parts of the neighborhoods, and generate \mathcal{P} -vertices in the union. Finally, we determine the dominating tail parts at every position x , and generate \mathcal{P} -vertices in the corresponding tail parts. Then, the simplices of the Palm distribution are those whose lowest mark \mathcal{P} -vertex is $(0, u)$.

With the model parameters set, the simulation framework gives us the opportunity to analyze the distribution of Δ_0 -degrees, Δ_1 -degrees and Δ'_0 -degrees of the generated finite networks with different network sizes by varying the intensities of the point processes. Specifically, to examine the finite-size effect on the distributions of the network properties of interest, we simulated 100 networks and kept the model parameters $\gamma = 0.7$, $\gamma' = 0.2$ constant, but altered the expected number λ and λ' of \mathcal{P} - and \mathcal{P}' -vertices, respectively. To examine the Palm distribution, we simulated 100 sets of 10 000 networks. In this case, the values of λ, λ' is indifferent, and we set them to $\lambda = \lambda' = 1$. Lastly, the parameter β was set so that the expected number of Δ_0 -degrees in the infinite network limit was 3.

As it was shown in Theorem 2.3, all the examined distributions exhibit a power-law tail in the infinite network limit. Thus, we fitted a power law distribution to the simulated values using the maximum likelihood method described in [2]. Determining the minimum value x_{\min} from which the power-law distribution should be fitted is not trivial. If we use lower values of x_{\min} , more data points can be considered for the fitting, resulting in a more robust fit of the power-law distribution, but the estimated power-law exponent is more biased as the power-law might not hold at lower values. Conversely, for higher values of x_{\min} , the estimated power-law exponent has less bias, but the fit is less robust as fewer data points are considered.

The boxplots of Figure 3 show how the fitted power-law exponents of the above-mentioned degree distributions fluctuate relative to the theoretical value derived for infinite networks in Theorem 2.3.

In the top row, we used $x_{\min} = 10$ for the fitting, while in the bottom row, we used $x_{\min} = 15$. It can be seen that the exponents in the top row fluctuate less but have a higher bias, while the exponents in the bottom row fluctuate more but have a lower bias. This is due to the fact that a set of \mathcal{P} -vertices form a simplex if they share a common \mathcal{P}' -vertex, and this more complex relationship between the \mathcal{P} - and \mathcal{P}' -vertices results in a higher variance of the estimated exponents. We can also see that the degree exponents fluctuate much more for the Δ'_0 -degree distribution than for the Δ_0 -degree distribution. This can be explained by the different decay rates of the neighborhoods of \mathcal{P} - and \mathcal{P}' -vertices: the power-law tails have exponents $1/\gamma = 1.43$ and $1/\gamma' = 0.5$, respectively, which results in fewer data points in the tail of the Δ'_0 -degree distribution compared to the Δ_0 -degree distribution. As it will be shown in Section 9, the Δ_0 - and Δ'_0 -degree distributions will be of particular interest when fitting the model parameters γ and γ' to the datasets. Analyzing the boxplots of the Δ_0 - and Δ'_0 -degree distributions, we can see that the power-law exponents of the degree distributions are close to the theoretical values derived for infinite networks above a network size of 10 000. Considering the optimal trade-off between bias and robustness, we chose to use $x_{\min} = 10$ for the fitting in the following sections.

Next, we analyze the distributions of the first Betti number by simulating 100 networks with fixed $\lambda = \lambda' = 100\,000$ and varying γ and γ' parameters. The histograms with fitted normal distributions and the corresponding Q-Q plots are shown in Figure 4. In alignment with Theorem 2.4, the Q-Q plots show that the Betti number is normally distributed for parameters $\gamma < 1/4$ and $\gamma' < 1/8$. The figures for $1/4 \leq \gamma \leq 1/2$

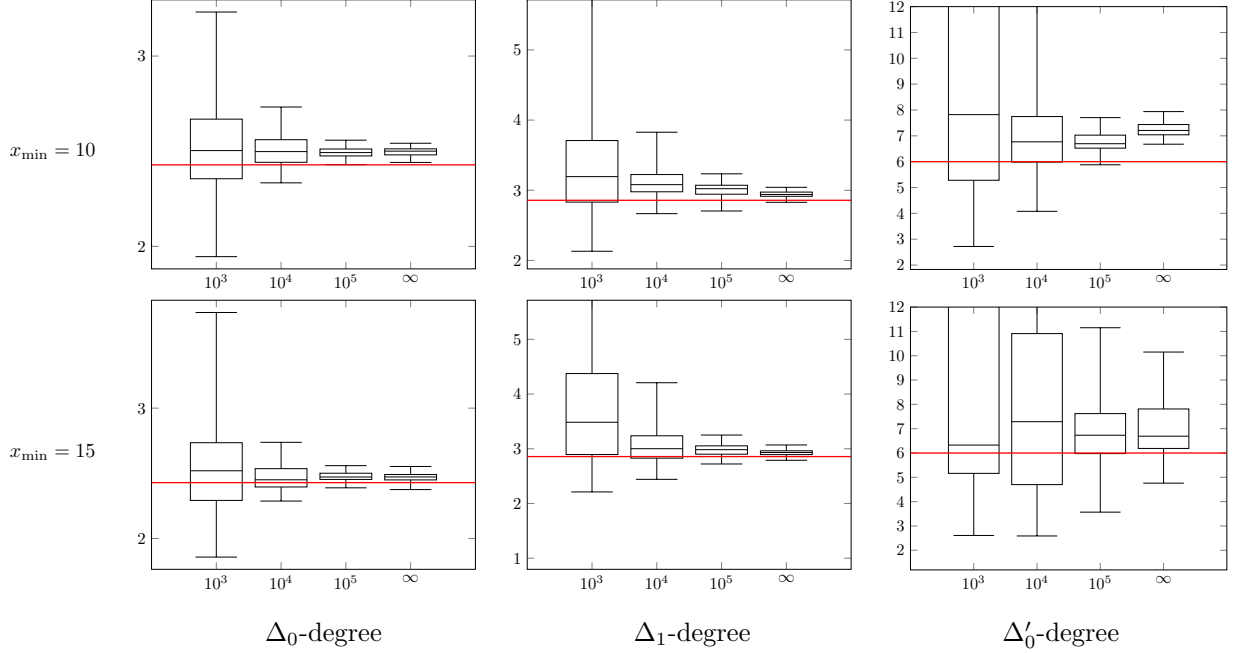


FIGURE 3. Fluctuation of the degree distribution exponents for different network sizes. The top row shows the power-law exponents when estimated from values larger than $x_{\min} = 10$, whereas the bottom row contains boxplots for the distribution of the exponents estimated from values larger than $x_{\min} = 15$.

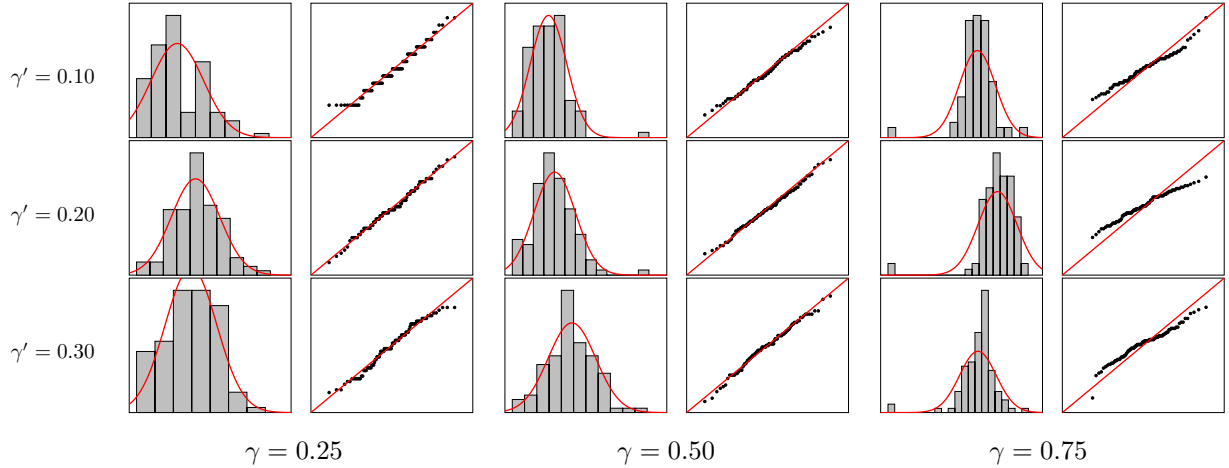


FIGURE 4. Distribution of the first Betti numbers with different γ and γ' parameters and $\gamma' \geq 1/8$ suggest that the normal distribution of the first Betti number also holds for these parameter ranges. The distribution of the Betti number for $\gamma = 0.75$, however, exhibit a fat left tail. Note that the leftmost bin of the histograms for $\gamma = 0.75$ are at 0, which means that some simulated networks did not contain any loops. This behavior can be explained by the presence of low-mark \mathcal{P} - and \mathcal{P}' -vertices that connect to many \mathcal{P}' - and \mathcal{P} -vertices when the edge count has an infinite variance, making the loops less likely to form. This observation leads to the conjecture that the Betti numbers have α -stable distributions if $\gamma > 0.5$.

Finally, we analyze the distribution of the number of edges and triangles in the simulated networks. As before, we simulated 100 networks with fixed $\lambda = \lambda' = 100\,000$ and varying γ and γ' parameters. The distribution of the edge counts are presented in Figure 5, where we fitted a normal distribution to the simulated values and visualized the corresponding Q-Q plots. As it was shown in Theorem 2.5 in the infinite

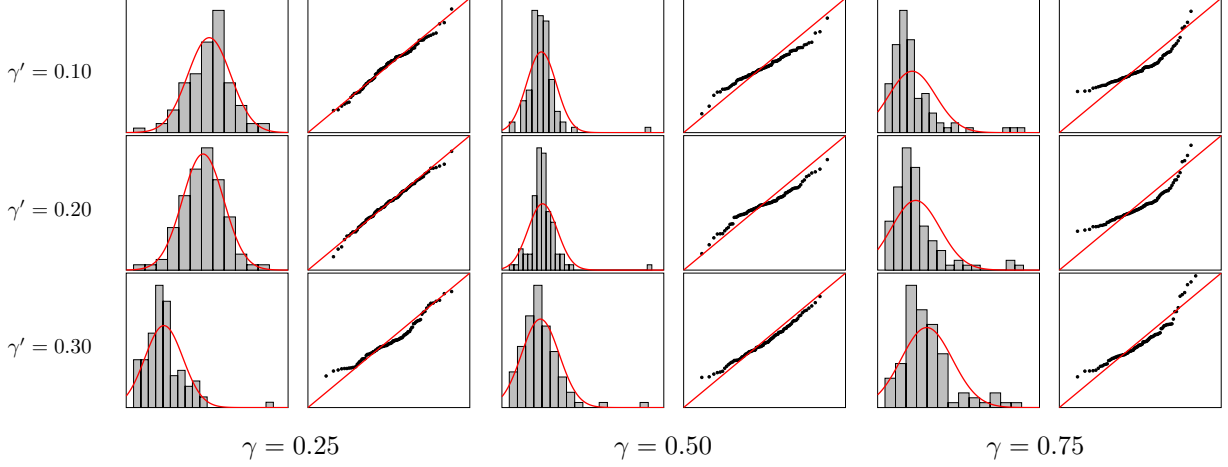


FIGURE 5. Distribution of edge counts with different γ and γ' parameters. For each combination of γ and γ' , we show the distribution of edge counts with the fitted normal distribution and the corresponding Q-Q plot.

network size limit, now the Q-Q plots show for finite networks that the number of edges are normally distributed for parameters $\gamma < 1/2$ and $\gamma' < 1/3$, and that the number of edges have an α -stable distribution if $\gamma > 1/2$ and $\gamma' \geq 1/3$. For $\gamma = 1/2$, it can be inferred from the Q-Q plots that the distribution of the number of edges is close to a normal distribution. The distribution of the triangle counts together with the fitted normal distributions and the Q-Q plots are shown in Figure 6. Again, the simulated distributions of finite networks are in alignment with Theorem 2.6: the Q-Q plots show that the number of triangles are normally distributed for parameters $\gamma < 1/2$ and $\gamma' < 1/5$. It is also clear from the Q-Q plots of Figure 6 that if $\gamma > 1/2$ and $\gamma' < 1/5$, the number of triangles has an α -stable distribution with $\alpha = 1/\gamma$, which was also shown for infinite networks in Theorem 2.6. We can furthermore conjecture that the number of triangles have an α -stable distribution if $\gamma' > 1/5$ irrespective of the value of γ .

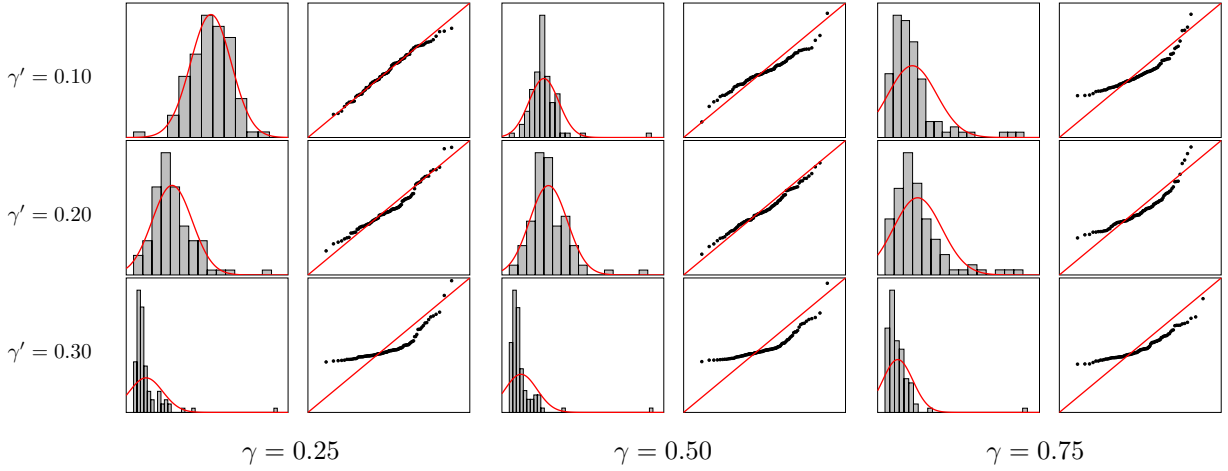


FIGURE 6. Distribution of triangle counts with different γ and γ' parameters. For each combination of γ and γ' , we show the distribution of triangle counts with the fitted normal distribution and the corresponding Q-Q plot.

After analyzing the degree distributions, the Betti numbers, and the number of edges and triangles in the simulated networks, we can conclude that the theoretical results derived for infinite networks hold for finite networks as well. We finish the simulation study by analyzing further degree distributions, which, although not of particular interest in the following sections, may be examined in a further study.

- The 0-coface degree distribution is the distribution of the number of edges incident to a \mathcal{P} -vertex.
- The 1-coface degree distribution is the distribution of the number of triangles incident to an edge.

As we will see in Section 9, these degree distributions exhibit a power-law tail in the datasets we analyze.

To examine the coface degree distribution of the networks generated by the model, we calculated the coface degree distributions for the sample network described at the beginning of Section 8. We also examined the fluctuations of the coface degree distribution exponents for different network sizes, and, as before, we simulated 100 networks with varying $\lambda = \lambda'$ intensities and fixed $\gamma = 0.7$ and $\gamma' = 0.2$ parameters. In this case again, we used $x_{\min} = 10$ for the fitting and set β so that $\mathbb{E}[\Delta_0^*] = 3$. The distributions of the 0- and 1-coface degrees and the fluctuations of the exponents are shown in Figure 7. We see that the distributions of the coface degrees are heavy tailed, and the power-law exponents of the distributions converge above a network size of 10 000.

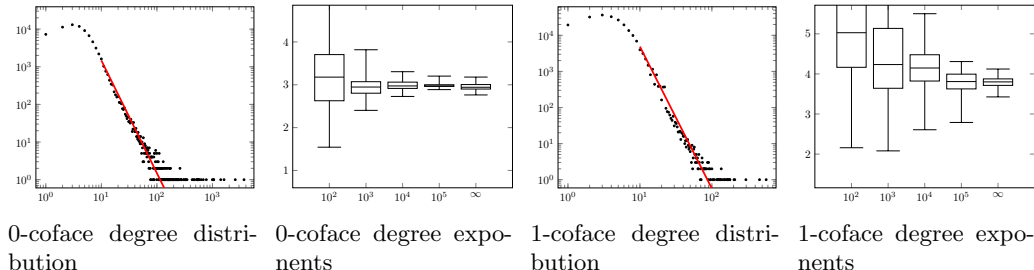


FIGURE 7. Typical coface degree distributions and the fluctuation of the power-law exponents for different network sizes. The power-law exponents were estimated from values larger than $x_{\min} = 10$.

9. ANALYSIS OF COLLABORATION NETWORKS

After the analysis of the finite-size effects in Section 8, we now compare our model with real-world datasets. To do so, we chose to analyze coauthorship networks, where the authors are represented by \mathcal{P} -vertices, and a \mathcal{P}' -vertex represents each of the publications.

Using the Python wrapper for the arXiv API, we collected all documents from the arXiv preprint server uploaded until 18 June 2024. Based on the label of the documents referring to their primary categories, we created four datasets for the four largest scientific fields, namely, **computer science**, **electrical engineering and systems science**, **mathematics**, and **statistics**, that we denote by **cs**, **eess**, **math**, and **stat**, respectively. In these datasets, we had access to the list of the author names of the documents. Identifying the authors by their names, we created

- a bipartite network where the \mathcal{P} -vertices are the authors and the \mathcal{P}' -vertices are the documents;
- a simplicial complex representing the higher-order network of the authors.

As simplicial complexes are closed under taking subcomplexes, each document with n authors is represented by $2^n - 1$ -simplices in the simplicial complex. This exponential dependence of the number of simplices on the number of authors led to an disproportionate influence of documents with a high number of authors on our results. To mitigate this effect, we included documents with at most 20 authors in our analysis, thereby neglecting a proportion of 0.13% of the documents.

The main properties of the datasets are summarized in Table 1.

TABLE 1. Main properties of the datasets

dataset	authors	documents	components	size of largest component
cs	504 959	540 573	23 909	439 375
eess	93 005	85 445	6 061	67 700
math	211 757	500 403	27 157	163 738
stat	48 700	40 869	4 236	36 094

Using the documents as \mathcal{P}' -vertices, we created a filtered simplicial complex for each of the datasets. We set the filtration value of a set of authors to be the number of papers they are all authors of, and used a filtration value decreasing from ∞ to 0 to create the filtered Dowker complex. We present in Figure 8 the persistence diagrams computed from the filtered Dowker complex. Although the datasets contain many components and loops, some of them have the same birth and death filtration values, leading to fewer points in the persistence diagrams.

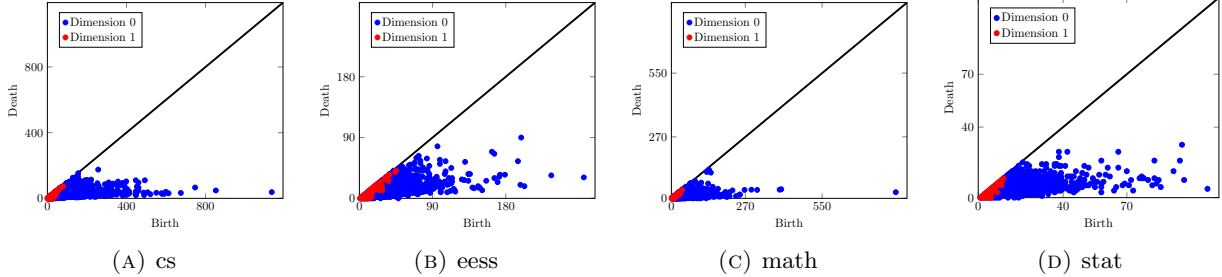


FIGURE 8. Persistence diagrams of the datasets.

Further properties of the datasets are illustrated in Figure 9. In the top row, we visualized the largest components of the datasets, where each document is represented by a polygon around the authors having a darker color if the document has more authors. Further rows show the degree distributions of the datasets together with the fitted power-law distributions. The degree distributions that we examine are similar as before in Section 8:

- The Δ_0 -degree distribution is the distribution of the number of documents an author is an author of.
- The Δ_1 -degree distribution describes the distribution of the number of documents of pairs of authors wrote together an author coauthored a document with.
- The distribution of the number of authors of a document is the Δ'_0 -degree distribution.

We see that all the visualized degree distributions are heavy-tailed, and the fitted power-law distributions describe the data well.

To compare the datasets with our model, we first need to estimate the model parameters. The γ and γ' parameters are estimated from the exponents of the fitted power-law distributions to the Δ_0 - and Δ'_0 -degree distributions, respectively.

Note that the datasets do not contain isolated \mathcal{P} - and \mathcal{P}' -vertices, i.e., authors without any documents and documents without any authors. Thus, we compensate for these in our model so that the numbers of authors and documents in the datasets match the number of non-isolated \mathcal{P} - and \mathcal{P}' -vertices in the simulations, respectively.

Let \mathcal{P}_0 and \mathcal{P}'_0 be the set of isolated \mathcal{P} - and \mathcal{P}' -vertices in the simulated simplicial complex, respectively, and let $p := (x, u) \in \mathcal{P}$ and $p' := (z, w) \in \mathcal{P}'$. Then, the expected number of non-isolated \mathcal{P} -vertices in the simulation is given by

$$\begin{aligned} \mathbb{E}[\#(\mathcal{P} \setminus \mathcal{P}_0)] &= \mathbb{E}\left[\sum_{p \in \mathcal{P}} \mathbb{1}\{\mathcal{P}'(B(p)) \neq 0\}\right] = \lambda \int_0^1 \mathbb{E}[\mathbb{1}\{\mathcal{P}'(B(p)) \neq 0\}] du \\ &= \lambda \int_0^1 1 - \mathbb{P}(\mathcal{P}'(B(0, u)) = 0) du = \lambda \int_0^1 1 - \exp(-\lambda'|B(0, u)|) du \\ &= \lambda \int_0^1 1 - \exp\left(-\lambda' \int_0^1 \int_{-\beta u^{-\gamma} w^{-\gamma'}}^{\beta u^{-\gamma} w^{-\gamma'}} dz dw\right) du = \lambda \left(1 - \int_0^1 \exp\left(-\frac{2\beta\lambda'}{1-\gamma'} u^{-\gamma}\right) du\right). \end{aligned}$$

After the application of the $\mu := 2\beta\lambda'/(1-\gamma')u^{-\gamma}$ substitution, we obtain

$$\mathbb{E}[\#(\mathcal{P} \setminus \mathcal{P}_0)] = \lambda \left(1 - \frac{1}{\gamma} \left(\frac{1-\gamma'}{2\beta\lambda'}\right)^{-\frac{1}{\gamma}} \int_{\frac{2\beta\lambda'}{1-\gamma'}}^{\infty} \mu^{-\frac{1}{\gamma}-1} e^{-\mu} d\mu\right) = \lambda \left(1 - \frac{1}{\gamma} \left(\frac{1-\gamma'}{2\beta\lambda'}\right)^{-\frac{1}{\gamma}} \Gamma\left(-\frac{1}{\gamma}, \frac{2\beta\lambda'}{1-\gamma'}\right)\right),$$

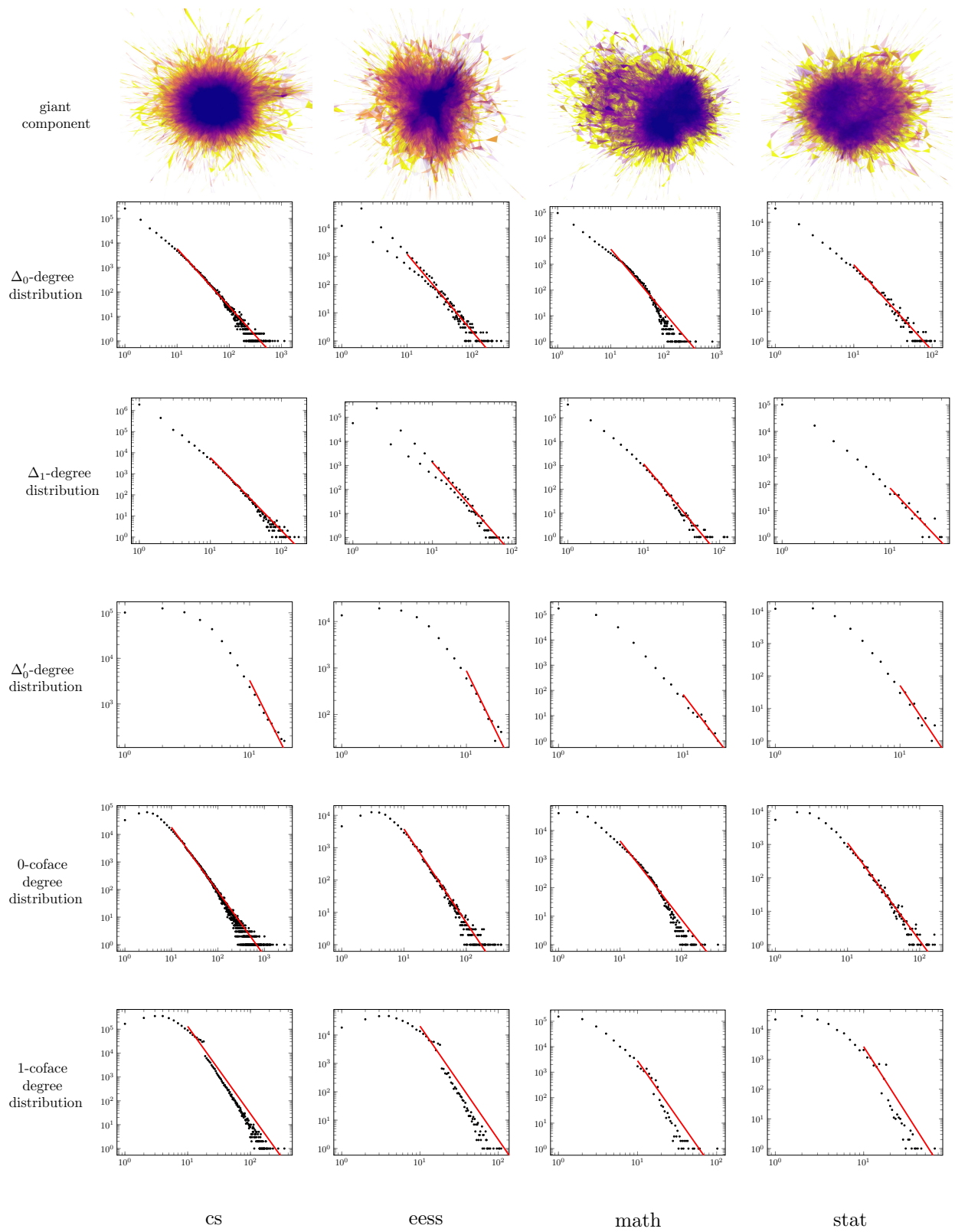


FIGURE 9. Main properties of the datasets

where Γ denotes the upper incomplete gamma function. Following the exact same steps, we find that the expected number of non-isolated \mathcal{P}' -vertices in the simulation is given by

$$\mathbb{E}[\#(\mathcal{P}' \setminus \mathcal{P}'_0)] = \lambda' \left(1 - \frac{1}{\gamma'} \left(\frac{1-\gamma}{2\beta\lambda} \right)^{-\frac{1}{\gamma'}} \Gamma \left(-\frac{1}{\gamma'}, \frac{2\beta\lambda}{1-\gamma} \right) \right).$$

Furthermore, we set the parameter β so that the expected number of edges in G^{bip} in the simulation matches the number of author–document edges in the datasets. Additionally, by the Mecke formula, we have

$$\mathbb{E} \left[\sum_{\substack{p \in \mathcal{P} \\ p' \in \mathcal{P}'}} \mathbf{1}\{p \in B(p')\} \right] = \int_{\mathbb{S}^2} \mathbb{P}(p \in B(p')) \, dp \, dp' = \frac{2\beta\lambda\lambda'}{(1-\gamma)(1-\gamma')}.$$

By numerically solving the above system of equations given by the expected number of non-isolated \mathcal{P} - and \mathcal{P}' -vertices, we obtain the parameter estimates shown in Table 2.

TABLE 2. Fitted power-law exponents and the inferred model parameters

dataset	Δ_0 -degree		\mathcal{P}' -vertex degree		β	λ	λ'
	exponent	γ	exponent	γ'			
cs	2.37	0.73	5.46	0.22	$8.19E-07$	579 719	532 491
eess	2.75	0.57	5.50	0.22	$7.89E-06$	98 528	83 985
math	2.44	0.69	6.51	0.18	$1.03E-06$	231 606	588 628
stat	2.89	0.53	5.74	0.21	$1.13E-05$	57 488	41 655

Using these parameters, we simulated a sample network for each of the datasets, which are visualized in Figure 10.

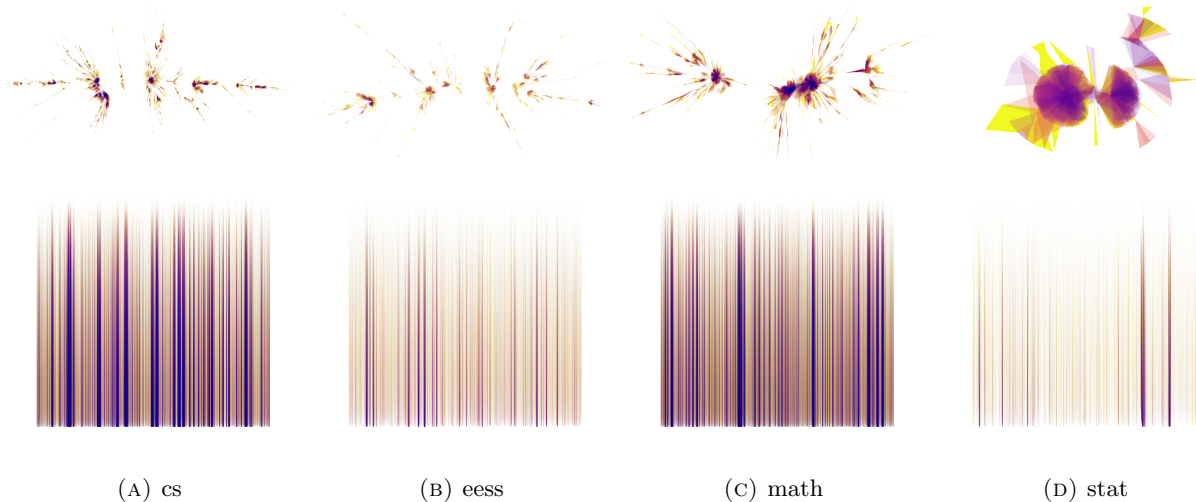


FIGURE 10. The largest component of the simplicial complexes built from the datasets

While the top row contains the largest components of the datasets, the bottom row shows the \mathcal{P} -vertices in the space \mathbb{S} . In both rows, similarly as above, each \mathcal{P}' -vertex is represented by a polygon around \mathcal{P} -vertices connecting to them with a darker color if the \mathcal{P}' -vertex is connected to more \mathcal{P} -vertices. We can see that the model networks possess a tree-like structure dominated by a couple of high-degree \mathcal{P} -vertices.

To determine if our model can capture the higher-order structures of the datasets, we need to performed hypothesis tests on the simplex counts and the first Betti number. Although Theorem 2.5 and our conjecture in Section 8 show that α -stable distributions describe the simplex counts and the first Betti number, it is not clear how to fully specify all parameters of these distributions. Therefore, we estimated the parameters of the α -stable distributions from the simulated networks to statistically compare the datasets with the networks

generated by the model. For each dataset, we simulated 100 networks, and fitted an α -stable distribution to the values with $\alpha = 1/\gamma$, which described the data well in all the cases.

The results of the hypothesis tests for the simplex counts and the first Betti numbers are summarized in Figure 11, and the parameters of the fitted distributions are shown in Tables 3, 4, and 5. Although the model parameters were set so that the expected number of Δ_0 -degrees in the simulation matches the number of author-document edges in the datasets, the hypothesis tests show that the higher-order structures of the datasets differ from that of the generated networks. The case of the eess and math datasets is particularly interesting, as in the case of the first, the simulated networks contain more triangles, but fewer edges compared to the datasets, while in the case of the latter, the opposite is true. In this case of the first Betti numbers, the values of the datasets are substantially larger than for the generated networks, and all the hypothesis tests are rejected. The reason for this deviation is that the simulated networks are dominated by a couple of high-degree \mathcal{P} -vertices resulting in a tree-like structure with relatively small number of loops, while the datasets contain more complex structures.

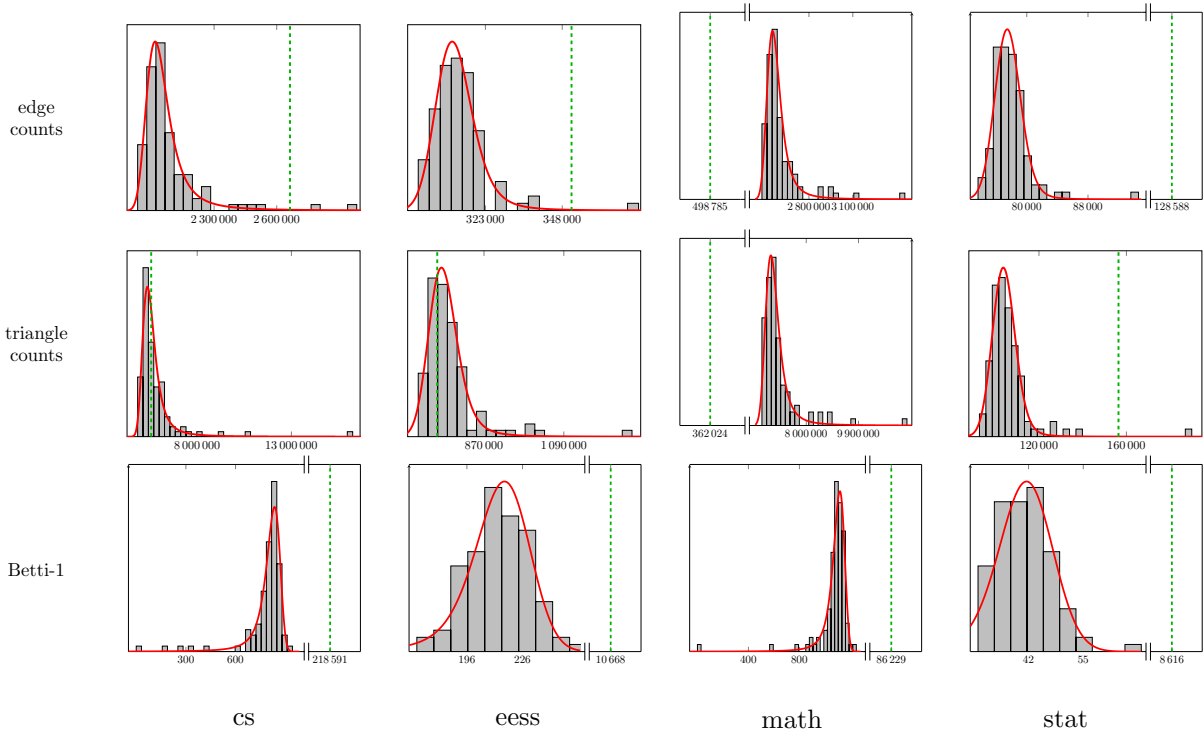


FIGURE 11. Hypothesis testing of the edge counts (top), triangle counts (center), and Betti-1 (bottom) for the datasets. The model parameters were determined based on the parameters of the datasets described in Table 2.

TABLE 3. Results of the hypothesis test for the edge counts

dataset	dataset value	$\hat{\alpha}$	$\hat{\beta}$	location	scale	p -value
cs	2 663 617	1.3658	1.0	2 093 994	43 104	$2.69E - 02$
eess	351 033	1.7506	1.0	314 266	4 331	$1.13E - 02$
math	498 785	1.4415	1.0	2 601 637	36 355	$0.00E + 00$
stat	128 588	1.8918	1.0	77 681	1 201	$1.73E - 04$

The results of the hypothesis tests show that although our model captured many properties of the datasets, it is too simplistic to accurately describe the higher-order structures of the datasets.

TABLE 4. Results of the hypothesis test for the number of triangles

dataset	dataset value	$\hat{\alpha}$	$\hat{\beta}$	location	scale	p -value
cs	5 556 409	1.3658	1.0	5 823 007	263 597	$9.13E - 01$
eess	741 063	1.7506	1.0	766 277	28 281	$6.50E - 01$
math	362 024	1.4415	1.0	6 973 583	187 554	$0.00E + 00$
stat	156 384	1.8918	1.0	104 413	3 720	$1.45E - 03$

TABLE 5. Results of the hypothesis test for the first Betti numbers

dataset	dataset value	$\hat{\alpha}$	$\hat{\beta}$	location	scale	p -value
cs	218 591	1.3658	-1.0	777	33	$0.00E + 00$
eess	10 668	1.7506	-1.0	211	11	$0.00E + 00$
math	86 229	1.4415	-1.0	1 069	35	$0.00E + 00$
stat	8 616	1.8918	-1.0	41	5	$0.00E + 00$

Acknowledgments. This work was supported by the Danish Data Science Academy, which is funded by the Novo Nordisk Foundation (NNF21SA0069429) and Villum Fonden (40516).

REFERENCES

- [1] A.-L. Barabási and R. Albert. Emergence of scaling in random networks. *Science*, 286(5439):509–512, 1999.
- [2] H. Bauke. Parameter estimation for power-law distributions by ML methods. *Eur. Phys. J. B*, 58:167–173, 2007.
- [3] C. Berge. *Graphs and Hypergraphs*. North-Holland Publishing Co., Amsterdam-London; American Elsevier Publishing Co., Inc., New York, 1973.
- [4] M. Brun and N. Blaser. Sparse Dowker nerves. *J. Appl. Comput. Topol.*, 3(1-2):1–28, 2019.
- [5] K. Choi. On medians of Gamma distributions and equations of Ramanujan. *Proc. Amer. Math. Soc.*, 121(1):245–251, 1994.
- [6] L. Decreusefond, M. Schulte, and C. Thäle. Functional Poisson approximation in Kantorovich-Rubinstein distance with applications to U -statistics and stochastic geometry. *Ann. Probab.*, 44:2147–2197, 2016.
- [7] D. Dereudre and M. D. Penrose. On the critical threshold for AB percolation. *J. Appl. Probab.*, 55(4):1228–1237, 2018.
- [8] H. Edelsbrunner and J. Harer. *Computational Topology: An Introduction*. American Mathematical Society, 2010.
- [9] J. D. Esary, F. Proschan, and D. W. Walkup. Association of Random Variables, with Applications. *Ann. Math. Statist.*, 38(5):1466 – 1474, 1967.
- [10] P. Gracar, A. Grauer, L. Lühtrath, and P. Mörters. The age-dependent random connection model. *Queueing Systems*, 93(3-4):309–331, 2019.
- [11] P. Gracar, M. Heydenreich, C. Mönch, and P. Mörters. Recurrence versus transience for weight-dependent random connection models. *Electron. J. Probab.*, 27:Paper No. 60, 31, 2022.
- [12] P. Gracar, L. Lühtrath, and P. Mörters. Percolation phase transition in weight-dependent random connection models. *Adv. Appl. Probab.*, 53(4):1090–1114, 2021.
- [13] Y. Hiraoka, T. Shirai, and K. Trinh. Limit theorems for persistence diagrams. *Ann. Appl. Probab.*, 28(5):2740–2780, 2018.
- [14] C. Hirsch and P. Juhász. On the topology of higher-order age-dependent random connection models. *arXiv preprint arXiv:2309.11407*, 2023.
- [15] S. K. Iyer and D. Yogeshwaran. Percolation and connectivity in AB random geometric graphs. *Adv. in Appl. Probab.*, 44(1):21–41, 2012.
- [16] J. Komjáthy and B. Lodewijks. Explosion in weighted hyperbolic random graphs and geometric inhomogeneous random graphs. *Stochastic Process. Appl.*, 130(3):1309–1367, 2020.
- [17] G. Last and M. D. Penrose. *Lectures on the Poisson Process*. Cambridge University Press, Cambridge, 2017.
- [18] M. D. Penrose. *Random Geometric Graphs*. Oxford University Press, Oxford, 2003.
- [19] M. D. Penrose. Continuum AB percolation and AB random geometric graphs. *J. Appl. Probab.*, 51A:333–344, 2014.
- [20] M. D. Penrose and J. E. Yukich. Central limit theorems for some graphs in computational geometry. *Ann. Appl. Probab.*, 11(4):1005–1041, 2001.
- [21] M. Reitzner and M. Schulte. Central limit theorems for U -statistics of Poisson point processes. *Ann. Prob.*, 41(6):3879–3909, 2013.
- [22] H. Samet. An overview of quadtrees, octrees, and related hierarchical data structures. In R. A. Earnshaw, editor, *Theoretical Foundations of Computer Graphics and CAD*, pages 51–68, Berlin, Heidelberg, 1988. Springer Berlin Heidelberg.
- [23] C. Siu, G. Samorodnitsky, C. L. Yu, and R. He. The many holes of preferential attachment—asymptotics of the expected Betti numbers of preferential attachment clique complexes. *arXiv preprint arXiv:2305.11259*, 2023.
- [24] C. Stegehuis and L. Weedage. Degree distributions in AB geometric graphs. *Phys. A*, 586:Paper No. 126460, 12, 2022.
- [25] R. van der Hofstad, P. van der Hoorn, N. Litvak, and C. Stegehuis. Limit theorems for assortativity and clustering in null models for scale-free networks. *Adv. Appl. Probab.*, 52(4):1035–1084, 2020.

- [26] R. van der Hofstad, P. van der Hoorn, and N. Maitra. Scaling of the clustering function in spatial inhomogeneous random graphs. *J. Stat. Phys.*, 190(6):110, 2023.
- [27] W. Whitt. *Stochastic-Process Limits*. Springer-Verlag, New York, 2002.

DEPARTMENT OF MATHEMATICS, UNIVERSITY OF BERGEN, BERGEN, NORWAY
Email address: `morten.brun@uib.no`

DEPARTMENT OF MATHEMATICS, AARHUS UNIVERSITY, AARHUS, DENMARK
Email address: `hirsch@math.au.dk`

DEPARTMENT OF MATHEMATICS, AARHUS UNIVERSITY, AARHUS, DENMARK
Email address: `peter.juhasz@math.au.dk`

DEPARTMENT OF MATHEMATICS, AARHUS UNIVERSITY, AARHUS, DENMARK
Email address: `otto@math.au.dk`